

## Model-Based Analysis of Biopharmaceutical Experiments To Improve Mechanistic Oral Absorption Modeling: An Integrated *in Vitro in Vivo* Extrapolation Perspective Using Ketoconazole as a Model Drug

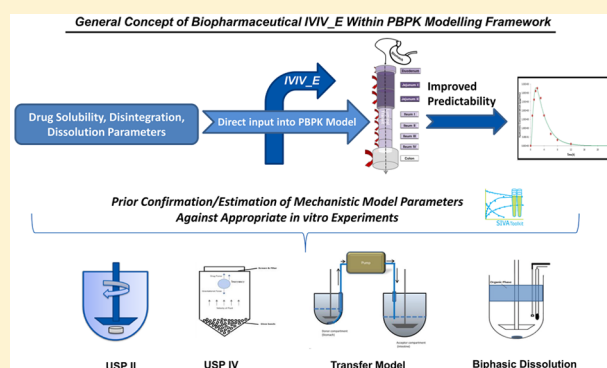
Shriram M. Pathak,<sup>\*,†</sup> Aaron Ruff,<sup>‡</sup> Edmund S. Kostewicz,<sup>‡</sup> Nikunj Kumar Patel,<sup>†</sup> David B. Turner,<sup>†</sup> and Masoud Jamei<sup>†</sup>

<sup>†</sup>Simcyp Limited (A Certara Company), Blades Enterprise Centre, John Street, Sheffield, S2 4SU, United Kingdom

<sup>‡</sup>Department of Pharmaceutical Technology, Johann Wolfgang Goethe University, Max-von-Laue-Strasse 9, Frankfurt am Main 60438, Germany

**ABSTRACT:** Mechanistic modeling of *in vitro* data generated from metabolic enzyme systems (viz., liver microsomes, hepatocytes, rCYP enzymes, etc.) facilitates *in vitro*–*in vivo* extrapolation (IVIV<sub>E</sub>) of metabolic clearance which plays a key role in the successful prediction of clearance *in vivo* within physiologically-based pharmacokinetic (PBPK) modeling. A similar concept can be applied to solubility and dissolution experiments whereby mechanistic modeling can be used to estimate intrinsic parameters required for mechanistic oral absorption simulation *in vivo*. However, this approach has not widely been applied within an integrated workflow. We present a stepwise modeling approach where relevant biopharmaceutics parameters for ketoconazole (KTZ) are determined and/or confirmed from the modeling of *in vitro* experiments before being directly used within a PBPK model. Modeling was applied to various *in vitro* experiments, namely: (a) aqueous solubility profiles to determine intrinsic solubility, salt limiting solubility factors and to verify pK<sub>a</sub>; (b) biorelevant solubility measurements to estimate bile-micelle partition coefficients; (c) fasted state simulated gastric fluid (FaSSGF) dissolution for formulation disintegration profiling; and (d) transfer experiments to estimate supersaturation and precipitation parameters. These parameters were then used within a PBPK model to predict the dissolved and total (i.e., including the precipitated fraction) concentrations of KTZ in the duodenum of a virtual population and compared against observed clinical data. The developed model well characterized the intraluminal dissolution, supersaturation, and precipitation behavior of KTZ. The mean simulated AUC<sub>0–t</sub> of the total and dissolved concentrations of KTZ were comparable to (within 2-fold of) the corresponding observed profile. Moreover, the developed PBPK model of KTZ successfully described the impact of supersaturation and precipitation on the systemic plasma concentration profiles of KTZ for 200, 300, and 400 mg doses. These results demonstrate that IVIV<sub>E</sub> applied to biopharmaceutical experiments can be used to understand and build confidence in the quality of the input parameters and mechanistic models used for mechanistic oral absorption simulations *in vivo*, thereby improving the prediction performance of PBPK models. Moreover, this approach can inform the selection and design of *in vitro* experiments, potentially eliminating redundant experiments and thus helping to reduce the cost and time of drug product development.

**KEYWORDS:** IVIV<sub>E</sub>, biopharmaceutics, PBPK, ketoconazole, dissolution modeling, precipitation, pharmacokinetics



### INTRODUCTION

Applications of physiologically based pharmacokinetic (PBPK) models are diverse, and they have been widely used in industry, academia, and regulatory agencies.<sup>1–4</sup> This interest is markedly reflected in the increased number of research publications on this topic<sup>5</sup> and their applications in regulatory submissions and recently approved drug labels,<sup>6</sup> regulatory guidance,<sup>7,8</sup> and concept papers.<sup>9</sup> PBPK models are also used in simulating the absorption processes specifically for optimizing formulations and drug products,<sup>10–13</sup> establishing mechanistic IVIVC,<sup>14,15</sup> predicting food effects,<sup>16–18</sup> and aiding justification of biowaivers.<sup>19–21</sup>

PBPK models facilitate the integration of two classes of information: (1) “System Data”, consisting of physiological, biological, and genetic characteristics of the species studied, and (2) “API Data”, consisting of the relevant physicochemical and disposition attributes of the compound and/or its dosage

**Special Issue:** Industry-Academic Collaboration in Oral Biopharmaceutics: The European IMI OrBiTo Project

**Received:** May 15, 2017

**Revised:** July 31, 2017

**Accepted:** August 3, 2017

**Published:** August 3, 2017

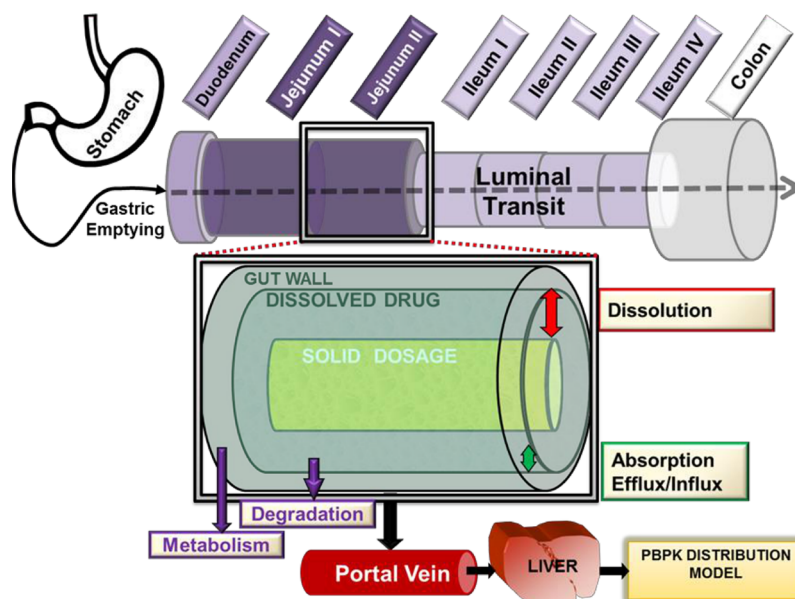


**Figure 1.** Schematic representation of the Advanced Dissolution, Absorption, and Metabolism (ADAM) model within the Simcyp population based simulator.

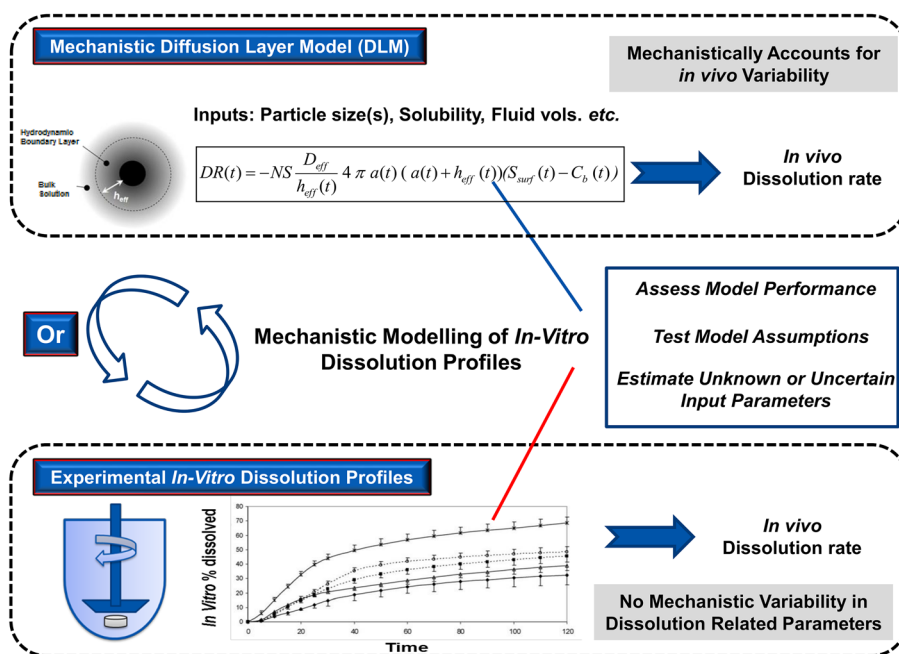


**Figure 2.** General concept of IVIV\_E using Simcyp *In Vitro* Analysis (SIVA) toolkit.

form.<sup>22</sup> In addition to reliable physiological data, the predictive performance of PBPK modeling depends strongly on drug-specific parameters.<sup>3</sup> Physiological/system-related parameters are typically curated, verified, and provided within databases as part of some commercial PBPK platforms; it is usually up to users to obtain the required drug-specific parameters.

Some drug-specific parameters are obtained from complex *in vitro* studies which typically rely on mechanistic model-based analysis of *in vitro* experimental results. For example, metabolic rates can be determined from various enzyme systems (viz., liver microsomes, hepatocytes, recombinantly expressed enzyme systems, etc.) and extrapolated to *in vivo* using *in vitro*–*in vivo* extrapolation (IVIV\_E) techniques, which play an important role in the successful prediction of *in vivo*

clearance.<sup>23–26</sup> Similar concepts can be applied to solubility and dissolution experiments in the form of mechanistic analysis of such assays to confirm and/or estimate intrinsic parameters required for mechanistic oral absorption simulations *in vivo*. However, this approach has not widely been applied within an integrated workflow.

The Advanced Dissolution, Absorption, and Metabolism (ADAM) model is a population-based mechanistic absorption modeling framework available within the Simcyp population-based PBPK simulator (Figure 1).<sup>16,27</sup> Generally, there are two ways to handle particle dissolution rates *in vivo* (Figure 2). First, the dissolution rates can be measured in “biorelevant” *in vitro* experiments (dissolution rate profile) and without adjustment directly used within the PBPK model or they can be modeled

mechanistically using a theoretical approach such as a diffusion layer model (DLM). In the latter case, drug solubility (both in bulk solution and within the particle surface microenvironment), particle size, bile-micelle partition, and a number of other particle-related parameters are considered explicitly. Once established and having gained confidence in the mechanistic model and its parameters (established by accurate prediction of experimental *in vitro* dissolution profiles) these can then be combined with physiological *system* parameters describing the gut luminal environment including pH, bile salt concentration, fluid volumes, and transit times to estimate the dissolution rate from drug particles within the various regions of the gastrointestinal (GI) tract. Thus, using a mechanistic model, such as the DLM, enables the simulator to account for regional and between-subject differences in the physiological parameters related to pH, bile salt concentration, and fluid volume dynamics in a mechanistic manner. Overall, this approach facilitates mechanistic translation of *in vitro* experiments to *in vivo* and enables the investigation of other factors such as food or even disease status impact on the absorption processes where the appropriate physiological data and mechanistic models are available.

The direct use of *in vitro* dissolution profiles as input to a PBPK model is available as noted above, but, without breaking down the *in vitro* information into its underlying mechanistic components, such an approach prohibits the incorporation of the known variability of physiological parameters into *in vivo* dissolution rate simulations which, particularly for BCS class II and IV drugs, may result in significant between-subject variability of dissolution rate unless attenuated through formulation strategies. Of course where *in vivo* variability of dissolution is known in advance not to be significant in terms of PK/PD outcomes, simpler approaches may be sufficient. Typically, *in vitro* dissolution assays are performed in conventional—USP I (basket apparatus), II (paddle apparatus), III (reciprocating cylinder apparatus), or IV (flow through)—apparatus and can in some circumstances quite closely simulate *in vivo* luminal conditions of the small intestine or stomach at least for a representative (“average”) individual. However, more generally, *in vitro* dissolution conditions are static and hence can only partially represent a particular location within the GI tract and perhaps then only over a short time frame due to time-dependent changes in *in vivo* fluid volumes (particularly in the proximal small intestine), absorption of dissolved drug, absorption of bile salt micelles in the distal small intestine, and other factors. Furthermore, these *in vitro* dissolution tests are not generally designed to account for the inherent between-subject physiological variability of luminal pH, luminal fluid volume, buffer capacity, bile salt concentration etc., to which the drug/dosage form is exposed during GI transit. Other differences between *in vitro* and *in vivo* conditions include, for example, the hydrodynamics (stirring rates, fluid flow patterns, etc.) and the lack of an absorptive component *in vitro*. It is important to emphasize that not all drugs, drug products, or doses of a given drug are likely to be sensitive to all of the aforementioned parameters. BCS class I drugs tend to be least sensitive to these factors and thus, in general, will not benefit from mechanistic modeling of dissolution. However, given that a high proportion of new drugs are BCS II or IV, there is a clear benefit to the use of mechanistic models to better characterize *in vivo* behavior where there is sensitivity to physiological conditions.

As a result of the factors discussed above, for many drug products, the direct use of *in vitro* dissolution profiles to estimate *in vivo* dissolution rates in PBPK models may not be appropriate. It is, therefore, desirable to confirm and/or estimate the required parameters of the mechanistic equations through modeling of *in vitro* experiments and then apply these models and parameters to *in vivo* simulations where the system parameters differ in general to those of the *in vitro* system, an approach we refer to as *in vitro*–*in vivo* extrapolation (*IVIV<sub>E</sub>*) of dissolution and solubility. Such biopharmaceutic *IVIV<sub>E</sub>* techniques rely on mechanistic understanding, appropriate experiments, and the modeling of *in vitro* dissolution profiles.

During luminal transit, the drug may undergo disintegration, dissolution, luminal degradation, supersaturation, precipitation, and redissolution. It is, however, not practical to mimic and therefore characterize all these complex processes in a single *in vitro* experiment. An alternative approach is to perform multiple, simpler independent experiments, each assessing relevant biopharmaceutic parameters of the drug product as required. These can then be combined in a mechanistic framework as discussed above.

Modeling of *in vitro* dissolution within the same mechanistic framework as that used for *in vivo* simulations provides three important benefits: (1) It allows assessment of the validity of the mechanistic dissolution model (the DLM in this case), and its assumptions, against a controlled and well-defined *in vitro* dissolution environment. This is otherwise difficult to assess in the complex *in vivo* luminal environment where dissolution is not directly measured. (2) It allows assessment of the quality and relevance of model input parameters such as solubility, particle size, disintegration rate, etc. (3) It can help to identify incorrect parameters or assumptions of the model. In such circumstances the user may choose to remeasure certain parameters (perhaps after additional sensitivity analysis) and/or estimate them using parameter estimation tools. A systematic *IVIV<sub>E</sub>* approach may therefore help to build confidence in the quality of the input parameters and mechanistic models (and their associated assumptions) before doing *in vivo* simulations with PBPK models, with the aim to improve predictive performance (Figure 2). This approach is intended to provide stepwise procedures to improve the quality of PBPK simulations; inadequate input parameters, deviation from model assumptions, and the use of parameters without support from appropriate *in vitro* experiments may adversely affect the interpretation of simulation results.<sup>28–30</sup>

To assess the performance of *IVIV<sub>E</sub>* and provide a proof of concept, we herein present a stepwise *in vitro* data modeling approach for ketoconazole (KTZ), a weakly basic drug known to precipitate *in vivo*, and its impact of *in vivo* predictions from a PBPK model. The performance of the proposed approach was assessed by comparing the predicted dissolved and total (precipitated and dissolved drug) concentration of KTZ (300 mg) in the duodenum with those reported from clinical studies. Predicted and reported plasma concentration time profiles were also compared.

## ■ MATERIALS AND METHODS

**Materials.** KTZ aqueous and biorelevant solubility data, the dissolution of Nizoral (ketoconazole) tablets in the USP-II apparatus, and its supersaturation/precipitation behavior using transfer experiments were determined at Goethe University (Ruff et al.<sup>31</sup>). Human *in vivo* duodenal luminal KTZ (300 mg) concentrations were reported by Psachoulis et al.<sup>42</sup>

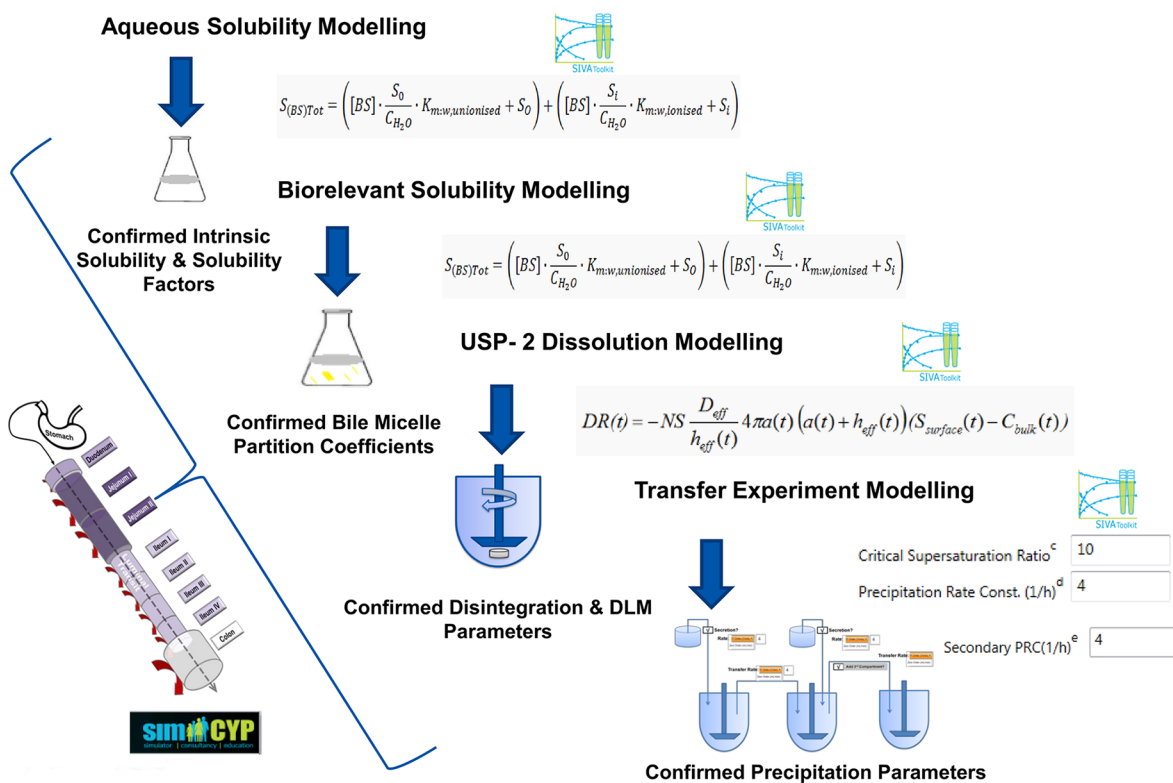
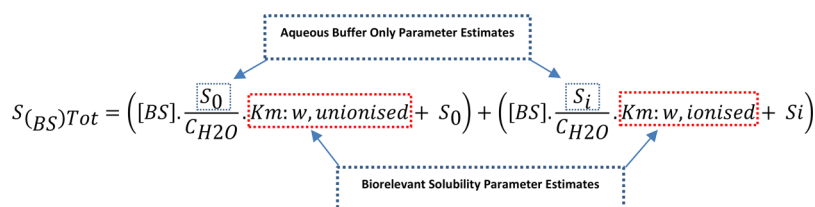


Figure 3. An integrated sequential *in vitro* modeling workflow followed within this research work.



**Stepwise IVIV\_E Approach.** Figure 3 graphically illustrates the stepwise IVIV\_E modeling approach undertaken in this study. First, intrinsic aqueous solubility ( $S_0$ , the solubility of un-ionized drug) and its salt limiting solubility factors (SFs; maximum solubility governed by the solubility product  $K_{sp}$ ) were characterized using the measured pH–solubility profile of KTZ. The consistency of the experimental pH–solubility profile with  $pK_a$ ,  $S_0$ , and the SF were also confirmed at this stage. Next, having fixed the aqueous phase parameters, the bile micelle:water partition coefficients ( $K_{m:w}$ ) for the ionized and un-ionized monomers were estimated through modeling of biorelevant solubility, i.e., in FaSSIF (fasted state simulated small intestinal fluid) and FeSSIF (fed state simulated small intestinal fluid). Solubility measurements at different pH and bile salt concentrations, obtained from the literature, were also used as an external validation of the estimated parameters. The formulation disintegration profile was established from the dissolution profile in FaSSGF at pH 1.6 in the USP II apparatus. KTZ is highly soluble at pH 1.6, and the dissolution profile is assumed to be disintegration controlled rather than controlled by dissolution rate of the API. Once the robustness of the mechanistic particle dissolution model parameters was confirmed in FaSSIF dissolution medium at pH 6.5 for an IR formulation, the transfer experiment data were modeled to

determine the first-order precipitation rate constant for the drug product studied. Finally, all these parameters, determined using *in vitro* experiments, were incorporated into the KTZ PBPK model. This approach facilitates combining the drug and formulation data with the relevant *in vivo* physiology rather than that of the *in vitro* experiments to simulate *in vivo* behavior. Each step is explained in detail below.

**Modeling Aqueous Solubility Data.** Equation 1 describes the overall structure of the solubility model used which is a composite function of aqueous phase solubility, governed by the Henderson–Hasselbalch equation for electrolytes and a bile micelle partition model accounting for micelle-mediated solubility of the API. The maximum aqueous phase solubility of ionized form of drug is also governed by the salt limiting solubility which is defined using the solubility factors (SFs). The mechanistic separation of the components of solubility enables calculation of free fraction and therefore the driving concentrations for permeation and precipitation models. It also enables individualized effective diffusion coefficients to be calculated for use in diffusion layer models of dissolution<sup>16</sup> when simulating populations with PBPK models.

In eq 1,  $[BS]$  is the concentration of bile salt (sodium taurocholate:lecithin molar ratio 4:1);  $S_0$  is the aqueous intrinsic solubility;  $S_{ionized}$  refers to the aqueous phase solubility



of the ionized form of the drug at a given pH (total aqueous phase solubility =  $S_0 + S_{\text{ionized}}$ );  $S(\text{BS})_{\text{Tot}}$  is the combined total solubility (aqueous at given pH and micelle mediated solubility at a stated [BS]);  $C_{\text{H}_2\text{O}}$  is the concentration of water (55.56 mM); and  $K_{\text{m:w,un-ionized/ionized}}$  are the bile micelle:water partition coefficients for neutral (or ionized) molecular species, respectively.

The equilibrium solubility of the unformulated (pure) KTZ in blank aqueous buffers—HCl/NaCl and maleate buffer—used in the preparation of biorelevant media, pH 2.0 FaSSGF-V2 and pH 6.5 FaSSIF-V2, respectively, was determined using HPLC (Table 1). These aqueous solubility measurements are

**Table 1. Aqueous and Biorelevant Solubility of KTZ<sup>a</sup>**

medium	solubility (mg/mL)
Aqueous Solubility	
HCl/NaCl buffer (pH 3.09)	11.573 ± 0.107
HCl/NaCl buffer (pH 3.48)	4.668 ± 0.042
maleate buffer (pH 6.52)	0.00424 ± 0.00010
HCl/NaCl (pH 2.0) + maleate buffer (pH 6.5) [250 mL:350 mL] (pH 5.81)	0.01951 ± 0.00014
Tris/maleate buffer solubility (pH 6.00)	0.012 ± 0.00042
Tris/maleate buffer solubility (pH 7.81)	0.0026 ± 0.00079
phosphate buffer solubility (pH 7.40)	0.00393
Biorelevant Solubility	
FaSSGF-V2 (pH 3.24)	10.622 ± 0.017
FaSSGF-V2 (pH 3.49)	4.908 ± 0.088
FaSSIF-V1 (pH 6.52)	0.02189 ± 0.00112
FeSSIF (pH 5.0)	0.576 ± 0.128
FaSSGF-V2 + FaSSIF-V2 (250 mL + 350 mL) (pH 5.77)	0.02446 ± 0.00015
FaSSGF-V2 + FaSSIF-V2 (250 mL + 500 mL) (pH 5.96)	0.01924 ± 0.00006

<sup>a</sup>Stated media pH values were not target pH values but were measured after the 24 h solubility experiment. Solubility is measured using pure (unformulated) API at 37 °C.

devoid of bile micelle-mediated solubility effects and hence were used for intrinsic solubility and SF verification within the solubility model. Moreover, the solubility measurements in aqueous phosphate buffer<sup>32</sup> and Tris/maleate buffer<sup>33</sup> were used for the external validation once the solubility parameters were established.

**Modeling Bile Micelle-Mediated Solubility.** A key parameter for defining micelle-mediated solubility is the micellar partition coefficient ( $K_{\text{m:w}}$ ), for which separate values can be defined for the neutral and charged forms of the drug. Initial estimates of  $K_{\text{m:w}}$  values can be obtained from a linear regression equation based upon  $\log P_{\text{o:w}}$  of the compound developed by Glomme et al.<sup>34</sup>

$$\begin{aligned} \log K_{\text{m:w,un-ionized}} &= a \log P_{\text{o:w}} + b \\ \log K_{\text{m:w,ionized}} &= a \log P_{\text{o:w}} + b - m_{\text{diff}} \end{aligned} \quad (2)$$

where  $a = 0.74$  and  $b = 2.29$  for sodium taurocholate/lecithin (4:1 ratio) mixtures and  $m_{\text{diff}}$  is a “rule-of thumb” correction factor for ionized drug partition; the default  $m_{\text{diff}}$  values (which serve as initial estimates) for mono- and dications are 1 and 2 respectively.<sup>35</sup>

At this stage,  $S_0$  and SF (eq 1), which were previously confirmed using aqueous only solubility measurements, were fixed and only the two  $K_{\text{m:w}}$  values were estimated using biorelevant solubility modeling (Figure 3). Hence biorelevant

media FaSSGF-V2 and FaSSIF-V2 solubility measurements were explicitly used for the estimation of the micelle:water partition coefficients for KTZ.

Such a model facilitates translating the *in vitro* determined micelle-mediated solubility parameters to *in vivo* allowing incorporation of the regional luminal pH and bile salt concentration in fasted and fed states and their interindividual variability within the PBPK framework.

**Modeling Formulation Disintegration.** During formulation disintegration it may be that disintegration is rate determining for the dissolution process and thus in general should be accounted for.<sup>36</sup> While disintegration for IR formulations may be sufficiently rapid as to be not significant in terms of clinical PK profiles, it may be of great importance to separate disintegration from API particle dissolution when assessing or parametrizing mechanistic models from *in vitro* dissolution experiments. Two of the doses modeled herein (discussed below) are IR dosage forms. KTZ has high solubility at the low gastric pH typical of the fasted state, and, therefore, formulation disintegration may be dissolution rate limiting; the solubility of KTZ in FaSSGF-V2 is very high (>10 mg/mL). Hence, we used the dissolution profile of Nizoral tablets from a FaSSGF-V2 medium in a USP 2 paddle apparatus to estimate a first-order disintegration rate constant using eq 3.

$$\begin{aligned} \% F_{\text{disint}} &= F_{\text{max}(\%)} [1 - e^{-K_{\text{d1}}(t - t_{\text{lag}})}] \quad \text{when } t > t_{\text{lag}} \\ \% F_{\text{disint}} &= 0 \quad \text{when } t \leq t_{\text{lag}} \end{aligned} \quad (3)$$

where  $\% F_{\text{disint}}$  is the percentage disintegrated at time  $t$ ,  $F_{\text{max}(\%)}$  is the maximum disintegration which was assumed to be 100% in this case,  $K_{\text{d1}}$  is the first-order disintegration rate constant ( $\text{h}^{-1}$ ), and  $t_{\text{lag}}$  is the lag time. This simple exponential function captured the *in vitro* dissolution profile in FaSSGF-V2 very well (AFE = 0.99).

**Modeling Precipitation Kinetics.** Experimental assessment of supersaturation and precipitation properties of drug products relevant to their *in vivo* behavior involves consideration of a multitude of factors, including rate and extent of drug solubilization in the gastric (donor) compartment, transfer rate, composition and volume of the simulated fluids, pH, bile salt concentration, bound and unbound micelle fraction, hydrodynamics (e.g., paddle RPM), ionization, permeation, and effect of formulation excipients.<sup>31</sup>

A number of dynamic *in vitro* models for studying intestinal precipitation have been developed with varying degrees of complexity.<sup>37</sup> Kostewicz et al. originally presented a transfer model in which a two compartment USP dissolution method is used corresponding to the stomach and first part of the small intestine, respectively;<sup>38</sup> subsequently, the original experimental setup underwent considerable improvements.<sup>31</sup> A wide range of physiologically relevant experimental parameters such as gastric emptying rate, hydrodynamics, GI pH, fluid volume, and bile salt concentration were taken into consideration before narrowing these down to the conditions of the current transfer experiment setup.

As a low  $\text{p}K_{\text{a}}$  weak base, KTZ may dissolve completely at fasted gastric pH but precipitate upon transit to the higher pH intestinal environment where it has much lower equilibrium solubility. Specifically, for this experiment the Nizoral tablet (200 mg) was placed in a 250 mL simulated gastric fluid (pH 2.0 FaSSGF-V2) compartment (donor phase), which was pumped into the 350 mL simulated intestinal fluid (pH 6.5

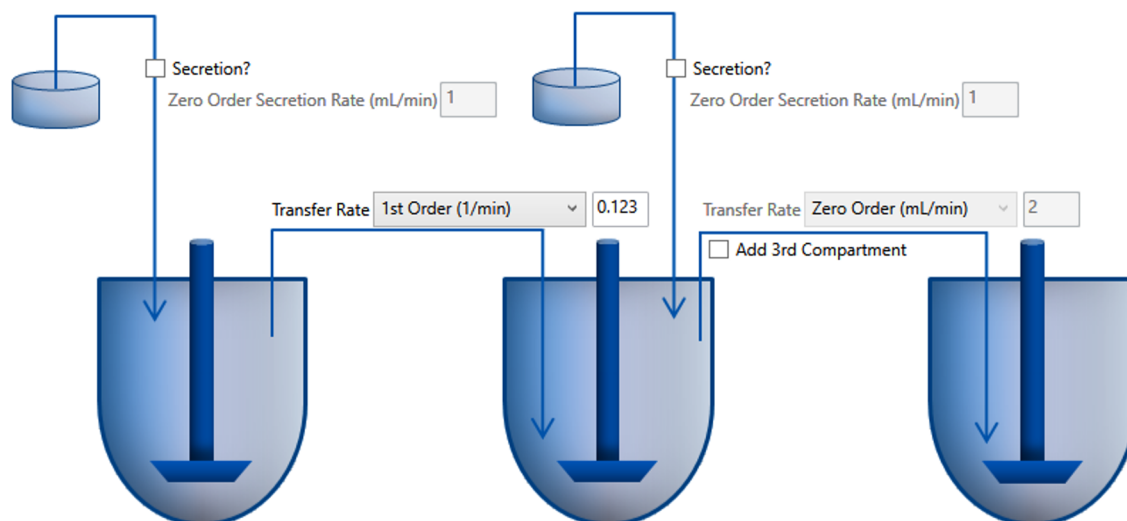


Figure 4. Details of transfer experiment module built into SIVA.

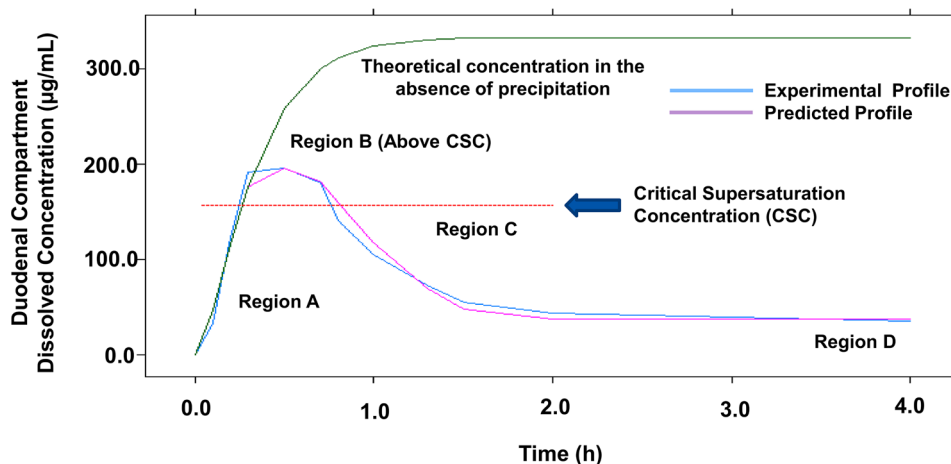


Figure 5. Schematic representation of first-order precipitation model built within the ADAM model.

FaSSIF-V2) compartment (acceptor phase) at a first-order rate constant of  $0.123 \text{ min}^{-1}$ .<sup>31</sup> The paddle rotation speed in both of the compartments was 100 rpm. The final pH, bile salt concentration, and volume in the acceptor phase vessel varied with the actual volume of donor phase transferred, and hence values were monitored at intervals during the experiment. These dynamic changes in model parameters (fluid volume, pH, and bile salt concentration) over time were accounted for as part of the mechanistic modeling of the transfer experiment results. Drug supersaturation and precipitation behavior in the acceptor compartment was modeled by analysis of the concentration versus time profile in the intestinal compartment, measured by a validated HPLC method.

The modeling of the *in vitro* experiment outcomes was carried out using the Transfer Module of the SIVA toolkit (Figure 4). There are reports of transfer experiments with varying donor and acceptor fluid volumes, paddle speeds (hydrodynamics), media composition, transfer rates, and also the number of compartments.<sup>37</sup> Recently, a transfer system with three compartments, representing the stomach, duodenum, and jejunum, was used to model the impact of disintegration on IR formulations of BCS I compounds.<sup>39</sup> The flexible options within the SIVA module thus not only help to model these varying experimental setups under one platform

but, in principle, can help scientists to design experiments. A database of library files defining the composition of widely used media (FaSSIF, FeSSIF, and simpler buffer systems) is provided which can be added to as required; in this study medium files were established representing donor (pH 2.0 FaSSGF) and acceptor (pH 6.5 FaSSIF-V2) media.

The pH and bile salt concentration within the donor compartment medium were assumed to remain static throughout the experiment (evaporation of the medium is considered to be negligible), and, as with the acceptor compartment, the medium is assumed to be well-stirred. The acceptor compartment pH was measured at the start (pH 6.50) and at the end of the complete transfer (pH 5.86) and then predicted at each sampling point dynamically using linear interpolation. The surfactant (in this case bile salt) concentration in the acceptor phase was recalculated at each time point during the simulations based on the volume of the donor phase transferred and the volume of the acceptor phase. Thus, thermodynamic solubility mediated by pH and [BS] were recalculated dynamically. However, measured pH and bile salt/surfactant concentrations at regular, shorter sampling intervals would be useful in the future.

The average dissolved concentration profile obtained from the replicate transfer experiments ( $n = 3$ ) was then fitted using

Table 2. Summary of Input Parameter Values Used for Ketoconazole Formulation Simulations in the Simcyp Simulator

parameter (units)	value used	refs/comments
Physchem and Blood Binding Parameters		
mol wt (g/mol)	531.4	
log $P_{o:w}$	4.04	ACD log $P_{o:w}$ (ChEMBL) <sup>64</sup>
compound type	diprotic base	Dollery et al. <sup>65</sup>
pK <sub>a</sub> (S)	2.94, 6.51	Dollery et al. <sup>65</sup>
fraction unbound in plasma	0.029	Martinez-Jorda et al. <sup>66</sup>
blood/plasma ratio	0.62	Simcyp inhibitor comp file
fraction unbound in enterocyte ( $f_{u_{gut}}$ )	0.06	Simcyp inhibitor comp file
Drug Absorption Parameters (ADAM Model)		
apparent Caco-2 cell permeability ( $\times 10^{-6}$ cm/s) apical pH 6.5–basolateral pH 7.4	15.1	Ingels et al. <sup>67</sup>
calibrator compounds Caco-2 cell permeability ( $\times 10^{-6}$ cm/s)	atenolol, 0.09 propranolol, 13.70 verapamil, 29.60	Ingels et al. <sup>67</sup>
predicted $P_{eff,man}$ ( $10^{-4}$ cm/s)	3.7612	predicted using the Caco-2 $P_{app}$ – $P_{eff,man}$ correlation model in ADAM
aq intrinsic solubility (mg/mL)	0.0034	back calculated using pH solubility data <sup>68</sup>
solubility factor (SF)	3403.823	estimated using SIVA
particle density (g/mL)	1.2	default value within ADAM
particle size distribution	monodispersed	assumed as data not available
particle radius ( $\mu$ m)	12	fitted based on <i>in vitro</i> profiles
log $K_{m:w}$ neutral	4.838	estimated using SIVA
log $K_{m:w}$ ion	4.124	
particle $h_{eff}$ prediction	Hintz–Johnson method	
CSR <sup>b</sup>	7.7	derived from the experimental data
PRC (1/h) <sup>b</sup>	1.8	
sPRC (1/h) <sup>b</sup>	1.64	estimated using SIVA
monomer diffusion coeff ( $10^{-4}$ cm <sup>2</sup> /s)	3.616	predicted within Simulator
micelle diffusion coeff ( $10^{-4}$ cm <sup>2</sup> /s)	0.78	Oh et al. <sup>69</sup>
Distribution Parameters		
model	full PBPK	
method	method 2 <sup>71</sup>	Cristofolletti et al. <sup>70</sup>
K <sub>p</sub> scalar	0.0115	
V <sub>ss</sub> (L/kg)	0.20	Cristofolletti et al. <sup>70</sup>
Elimination Parameters		
CL <sub>po</sub> (L/h)	12.5 and 7.4 (with CV = 40%) (for 200 and 400 mg doses, respectively)	PK nonlinear, after Huang et al. <sup>51,70</sup>
hepatic uptake scalar	2.07	Simcyp inhibitor comp. file
renal clearance (L/h)	0.147	after Huang et al. <sup>51</sup>

<sup>a</sup>ChEMBL Database (<https://www.ebi.ac.uk/chembl/compound/inspect/CHEMBL75>). KTZ enzyme inhibition (CYP2C8, CYP2C9, CYP3A4, and CYP3A5) parameters are also available as part of the Simcyp compound file, but this study does not consider DDIs, so the associated values have not been reported here. See also main text. <sup>b</sup>First-order precipitation model parameters: critical supersaturation ratio (CSR); precipitation rate constant (PRC) and secondary precipitation rate constant (sPRC).

built-in parameter estimation (PE) tools to estimate the precipitation parameters of an empirical first-order model, namely, the critical supersaturation ratio (CSR), precipitation rate constant (PRC), and (an optional) secondary PRC (sPRC). The CSR specifies the maximum extent of supersaturation of a drug in solution and is the ratio of the critical supersaturation concentration (CSC, sometimes referred to as the Kinetic “Solubility”) to the equilibrium solubility at a given pH and [BS] (region A, Figure 5). Precipitation can only start once the CSC is reached: this is one way in which the model is able to accommodate a lag time between the onset of supersaturated conditions and the onset of precipitation. The rate of precipitation is governed by the PRC (regions B and C, Figure 5). Where a single PRC is insufficient to capture the concentration time profile, the sPRC can be activated (region B only; i.e., when the dissolved concentration reaches or exceeds the CSC). Once the concentration drops below the CSC again,

the PRC (alone) is applied until the concentration reaches the equilibrium solubility (region D). This model is not intended to capture the underlying processes determining the shape of the concentration time profile. In particular, there may be a variety of mechanisms determining the observed concentrations within region B including nucleation, a metastable liquid–liquid phase separation (LLPS),<sup>40</sup> and transfer of dissolved drug from the donor to the receptor compartment (and also out of the compartment were a 3 compartment system to be used). Where the plateau region (B) concentration remains stable for an extended period, the sPRC may be activated and assigned a very low value effectively providing an additional lag time prior to precipitation. More mechanistic models could be developed (parametrized) to better capture these processes, but these would require additional experimental measurements to be made in the *in vitro* studies such as, for example, identification and characterization of LLPS, knowledge of amorphous

solubility, detection of the onset of particle growth, monitoring of particle size distributions over time, etc., which were not available for this study.

The KTZ intrinsic solubility ( $S_0$ ), bile micelle partition coefficients ( $K_{m,w}$  values), and tablet disintegration parameters estimated in the previous modeling steps were fixed at this stage. Particle size distribution (PSD) for the IR dosage forms is not available in the public domain. Hence PSD was assumed to be monodispersed and particle radius was manually fitted to 12  $\mu\text{m}$  based on modeling of multiple *in vitro* dissolution profiles. The drug parameters not readily available experimentally were calculated using built-in models within the Simcyp Simulator (*viz.*, monomer diffusion coefficients) as reported in Table 2. The particle density ( $\rho$ ) was assigned a software default value within the model ( $\rho = 1.2 \text{ g/mL}$ ); sensitivity analysis was performed for this parameter, and within typical ranges encountered with API (1.0 to 1.3  $\text{g/mL}$ )  $\rho$  does not have a significant impact on predicted profiles.

**Modeling of Particle Dissolution.** As described in the previous section, the dissolution of Nizoral tablets (200 mg) was tested in simulated gastric fluid where the solubility of KTZ was very high and disintegration of the drug dosage form was assumed to be rate limiting for dissolution. In order to assess the model and its parameters for handling fine particle dissolution (required for the *in vivo* simulations) the tablet dissolution data published by Galia et al.<sup>41</sup> was analyzed. The dissolution of Nizoral tablets in a medium simulating the small intestinal content in the fasted state (pH 6.5 FaSSIF) was used; the experiments were performed in the USP II paddle apparatus at 100 rpm with 500 mL of medium (Table 3).

**Table 3. Summary of the Experimental Conditions Followed in *in Vitro* Dissolution Studies**

setup parameter	dissolution study	
	FaSSGF	FaSSIF
medium used	pH 2.0 FaSSGF	pH 6.5 FaSSIF
medium vol (mL)	250	500
temp ( $^{\circ}\text{C}$ )	$37 \pm 0.5$	$37 \pm 0.5$
paddle speed	100 rpm	100 rpm
dosage form	Nizoral 200 mg tablet	Nizoral 200 mg tablet

The estimated parameters from previous experiments were used in the diffusion layer model (eq 4), and the model simulations were compared with extracted literature data.

$$\text{DissRate}(t) = -NS \frac{D_{\text{eff}}}{h_{\text{eff}}(t)} 4\pi a(t) (a(t) + h_{\text{eff}}(t)) (S_{\text{surface}}(t) - C_{\text{bulk}}(t)) \quad (4)$$

where  $N$  is the number of particles (in a given particle size bin for polydispersed formulations),  $S$  is empirical scalar (default value 1),  $D_{\text{eff}}$  is the effective diffusion coefficient,  $a(t)$  is particle radius at time  $t$ ,  $h_{\text{eff}}(t)$  is the effective diffusion layer thickness at time  $t$ ,  $S_{\text{surface}}(t)$  is the concentration of drug at the particle surface at time  $t$ , and  $C_{\text{bulk}}(t)$  is the concentration of the drug in the bulk solution at time  $t$ .

**Integration of the Estimated Model Parameters within PBPK Framework.** To evaluate the proposed *IVIV\_E* approach, the model parameters evaluated and/or estimated in the various *in vitro* experiments (Table 1) (*viz.*, solubility, disintegration/dissolution, and supersaturation/precipitation values) were integrated into a human population PBPK model. The model was used to simulate plasma

concentration profiles in healthy Caucasian individuals, and the predicted dissolved and total duodenal concentrations were compared to those reported for 12 subjects studied in the clinic (Psachoulias et al.<sup>42</sup>). The simulations are repeated with 10 different sets of 12 individuals in order to assess the impact of interindividual variability (sample size) on the interpretation of the outcomes. All simulations were performed using the Simcyp Population Based Simulator (Version 15 Release 1, Simcyp Ltd., Sheffield, U.K.). The simulator separates information based on the system (*i.e.*, human body) from those of the drug and the study design parameters (*e.g.*, dose, subject number, duration of study, fasted/fed state, etc.). The “System Data”, in the form of population libraries built from extensive analyses of demographic, anatomic, genetic, and tissue-specific characteristics of a population, was used as a basis to generate virtual healthy subjects. The virtual trials were built to mimic as closely as possible the clinical study design (Psachoulias et al.<sup>42</sup>) in terms of dose, study duration, proportion of males and females, age range, fluid intake with administered dose, and clinical sampling times (Table 4).

**Table 4. Clinical Trial Design Parameters Used in the Simulation Studies**

parameter	Psachoulias et al. <sup>42</sup>	Mannisto et al. <sup>49</sup>	Daneshmend et al. <sup>64</sup>	Huang et al. <sup>57</sup>
dose (mg)	300	200	200 and 400	200
formulation	solution	IR-tablet	IR-tablet	IR-tablet
population	Sim-Healthy Volunteers (Simcyp Simulator)			
sample size	10 trials $\times$ 12	10 trials $\times$ 10	10 trials $\times$ 8	10 trials $\times$ 24
study duration (h)	1.2	24	32	48
age range (years)	20–38	22–26	20–31	18–25
proportion of females	0.17	0.50	0.63	0
fluid intake with dose (mL)	240	100	100	200
site of ref concns	duodenal fluids		plasma	

The model performance was evaluated by comparing the area under the total and dissolved duodenal concentration time profiles ( $\text{AUC}_{0-t}$ ), precipitated fraction, and overall shape of the duodenal profiles of the observation and prediction. The precipitated fraction in the simulated aspirate,  $\pi_{\text{lumen}}$ , was estimated by eq 5 per Psachoulias et al.<sup>42</sup> The mean precipitated fraction was estimated using the average precipitated fractions up to 30 min post administration ( $n = 120$ ) and then calculating the overall mean of these averages.

$$\pi = 1 - \frac{C}{C_t} \quad (5)$$

where  $C$  is the concentration of the dissolved drug and  $C_t$  is the total amount of drug (dissolved and precipitated) per unit fluid volume.

**Model Performance for the Prediction of Plasma Concentration–Time Profiles.** Psachoulias et al.<sup>42</sup> evaluated the precipitation behavior of KTZ in GI luminal fluid samples; however, the clinical study did not involve assessing the systemic exposure of the drug in the same volunteers; dual duodenal and plasma sampling has been reported in recent study protocols such as with posaconazole,<sup>43</sup> which provides additional simultaneous reference concentrations for assessing PBPK model performance. Therefore, in order to further



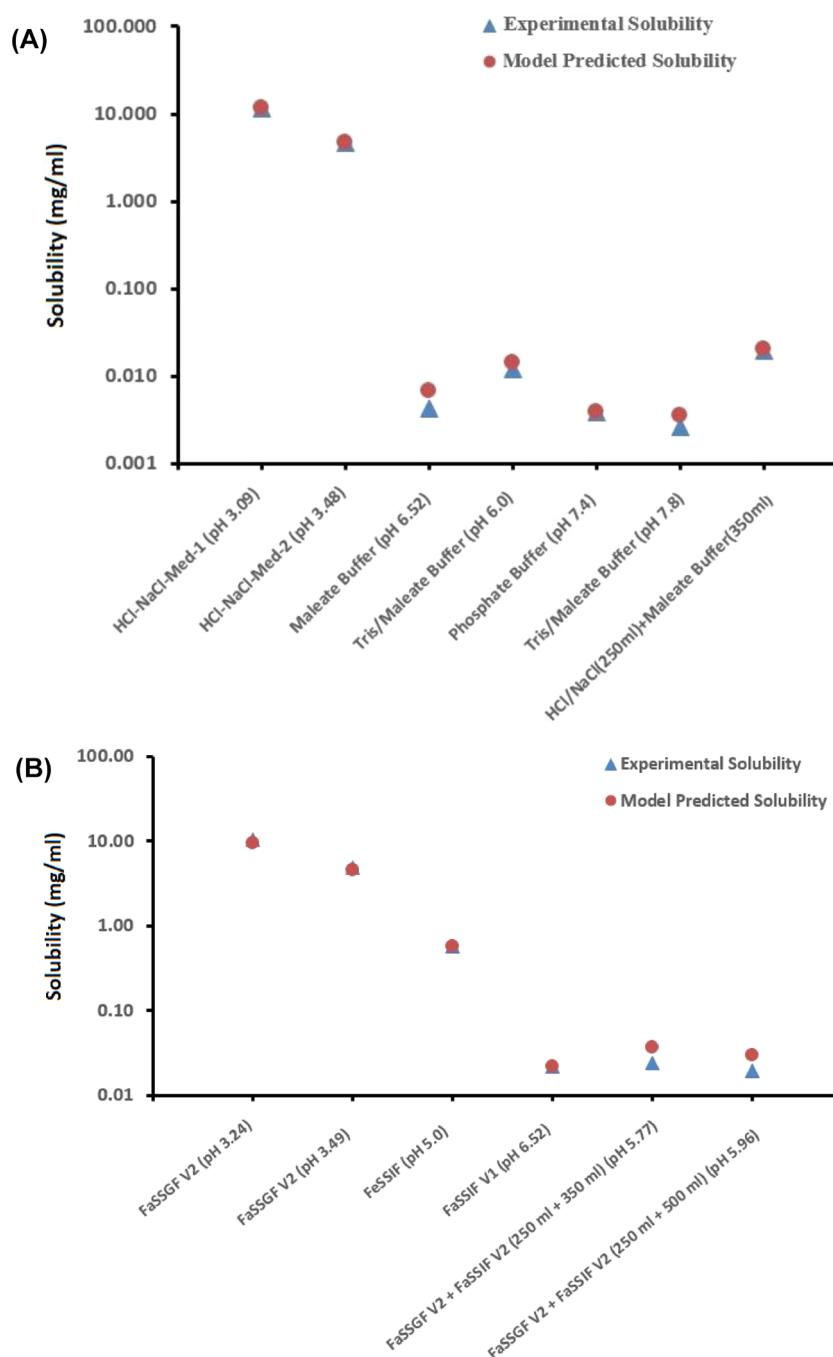


**Figure 6.** (A) KTZ aqueous solubility modeling results. (B) KTZ biorelevant solubility modeling results.

validate the model, additional human clinical studies (immediate release oral doses ranging from 200 to 400 mg) were identified from the published literature, simulated with the appropriate trial design, and compared via plasma concentration time profiles (Table 4). Parameters determined through the use of the stepwise, mechanistic modeling of *in vitro* pharmaceutical experiments along with physicochemical, protein and blood binding, permeability, and metabolism parameters of KTZ, collated from the literature, were integrated within the PBPK model (Table 2). However, with the limited information on the formulations used in these studies (dating from the period 1982–1986) and inconsistent disintegration results reported *in vitro*,<sup>41,44–48</sup> disintegration was assumed to be negligible in these additional simulation trials. As with the

simulations of the study of Psachoulis et al.,<sup>42</sup> ten independent virtual trials, each with the number of subjects used in the associated clinical study, were simulated in each case in order to make an assessment of the representativeness of a single trial in relation to interindividual variability. The predictive performance of the model was then assessed by comparing the predicted to the observed PK profiles reported in the literature studies.<sup>49–51</sup>

## RESULTS

**Aqueous and Biorelevant Solubility Modeling.** The aqueous solubility modeling confirmed the intrinsic solubility of KTZ as 0.0034 mg/mL while the SF was estimated to be 3404. The estimated aqueous solubility parameters were successfully

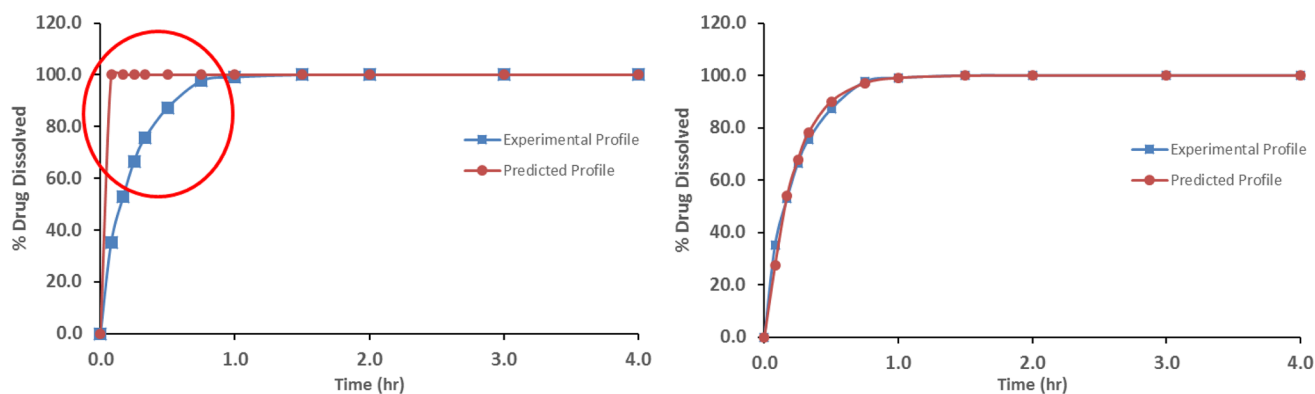


**Figure 7.** Modeling disintegration parameters of KTZ in pH 2.0 FaSSGF-V2 medium, without (left) and with (right) a formulation disintegration function.

used to predict the KTZ solubility in aqueous phosphate and Tris/Maleate buffer which were not used at the fitting stage (Figure 6A). Observed vs model predicted values were as follows: 0.012 mg/mL vs 0.0144 mg/mL in Tris/maleate pH 6.0 buffer, 0.00394 mg/mL vs 0.00384 mg/mL in phosphate pH 7.4 buffer, and 0.026 mg/mL vs 0.0036 mg/mL in Tris/maleate pH 7.8 buffer.

The aqueous phase solubility parameters having been established, the bile-micelle partition coefficients were assessed using biorelevant solubility measured in FaSSGF-V2 (pH 3.24; pH 3.49), FaSSIF, and FeSSIF media. Bile-micelle partition coefficients predicted from the built-in  $\log P_{o,w}$  model were not sufficiently predictive when used in eq 1 to predict total solubility and were, therefore, estimated (Figure 6B); fitted  $\log K_{m,w}$  values were 4.838 and 4.124 for neutral and ionized monomers, respectively. The external predictability of the model was also confirmed using the solubility of the KTZ in mixture of the buffers: FaSSGF-V2 + FaSSIF-V2 (250 mL + 350 mL) with final pH of 5.77 and bile salt concentration of 1.75 mM and FaSSGF-V2 + FaSSIF-V2 (250 mL + 500 mL) with final pH of 5.96 and bile salt concentration of 2.026 mM.

**Disintegration Model Parametrization.** The diffusion layer model (DLM) alone could not correctly predict the dissolution of the tablet in the FaSSGF-V2 medium without accounting for the disintegration process (Figure 7). The results clearly underline the importance of accounting for disintegration which, while sometimes not significant in terms of PK outcomes *in vivo*, can significantly bias assessment of the DLM against *in vitro* experimental results. Fitting the release profile of the drug in the medium using a first-order disintegration function gave an  $F_{max}$  of 100%,  $K_{d1}$  of 0.079  $h^{-1}$ , and  $t_{lag}$  of zero. These parameters were then used to characterize the disintegration of KTZ tablet in the donor compartment of the subsequent transfer experiment.

**External Validation for the Assessment of the Particle Dissolution Model.** To further assess the model performance we also evaluated its ability to predict *in vitro* FaSSIF dissolution data of 200 mg Nizoral tablets reported by Galia et al.; Figure 8 graphically illustrates the simulated and experimental profiles which are in good agreement (AFE = 1.01). The dissolution of the Nizoral tablet is solubility limited *in vitro*, and only 6.01% of the drug dissolved in the medium, which corresponds to an apparent KTZ solubility of  $\sim 0.024$  mg/mL in FaSSIF. This value is very close to the reported FaSSIF solubility of unformulated KTZ, viz.,  $\sim 0.022 \pm 0.001$  mg/mL. Hence, it seems reasonable to assume that formulation

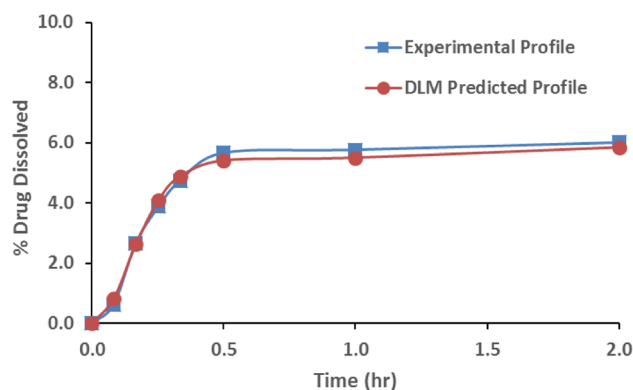


**Figure 8.** pH 6.5 FaSSIF dissolution data modeling using a mechanistic diffusion layer model (DLM) within the ADAM model.

excipients did not have a significant impact on drug solubility in this study. Therefore, the API solubility parameters established previously are expected to be relevant for modeling the dissolution of the API particles in Nizoral IR tablets.

**In Vitro Model Performance: DLM and Precipitation Model.** The concentration profile of the dissolved KTZ in the acceptor phase of the transfer experiment was modeled using a first-order precipitation model (Figure 8). The observed and the predicted profiles were also compared against the theoretical concentration profiles predicted considering the concentration of dissolved KTZ transferred into the acceptor phase, the transfer rate, and thereby the dilution effect, but assuming “no precipitation”. The maximum KTZ concentration reached and the corresponding equilibrium solubility of KTZ in the diluted acceptor phase medium (FaSSGF-V2:FaSSIF-V2, 250:350) were used to calculate CSR (7.7) and PRC ( $1.8 h^{-1}$ )<sup>31</sup> and were a direct input into the SIVA model. The SIVA Toolkit was then used to estimate the sPRC ( $1.64 h^{-1}$ ) for KTZ. A fifth-order Runge–Kutta method was used to solve the ordinary differential equations with an integration error tolerance of 0.001.

**The PBPK Model Performance.** The KTZ parameters, assessed and, where required, estimated through modeling of *in vitro* experimental data, were incorporated into the PBPK model, which was used to predict the duodenal fluid concentration profiles in 120 individuals (10 trials with 12 volunteers as described above). The simulated values compared favorably to the clinical values (Figures 9A and 9B). The mean predicted AUC of the total duodenal ( $513.76 \mu g h mL^{-1}$ ) and dissolved duodenal concentration ( $421.90 \mu g h mL^{-1}$ ) profiles

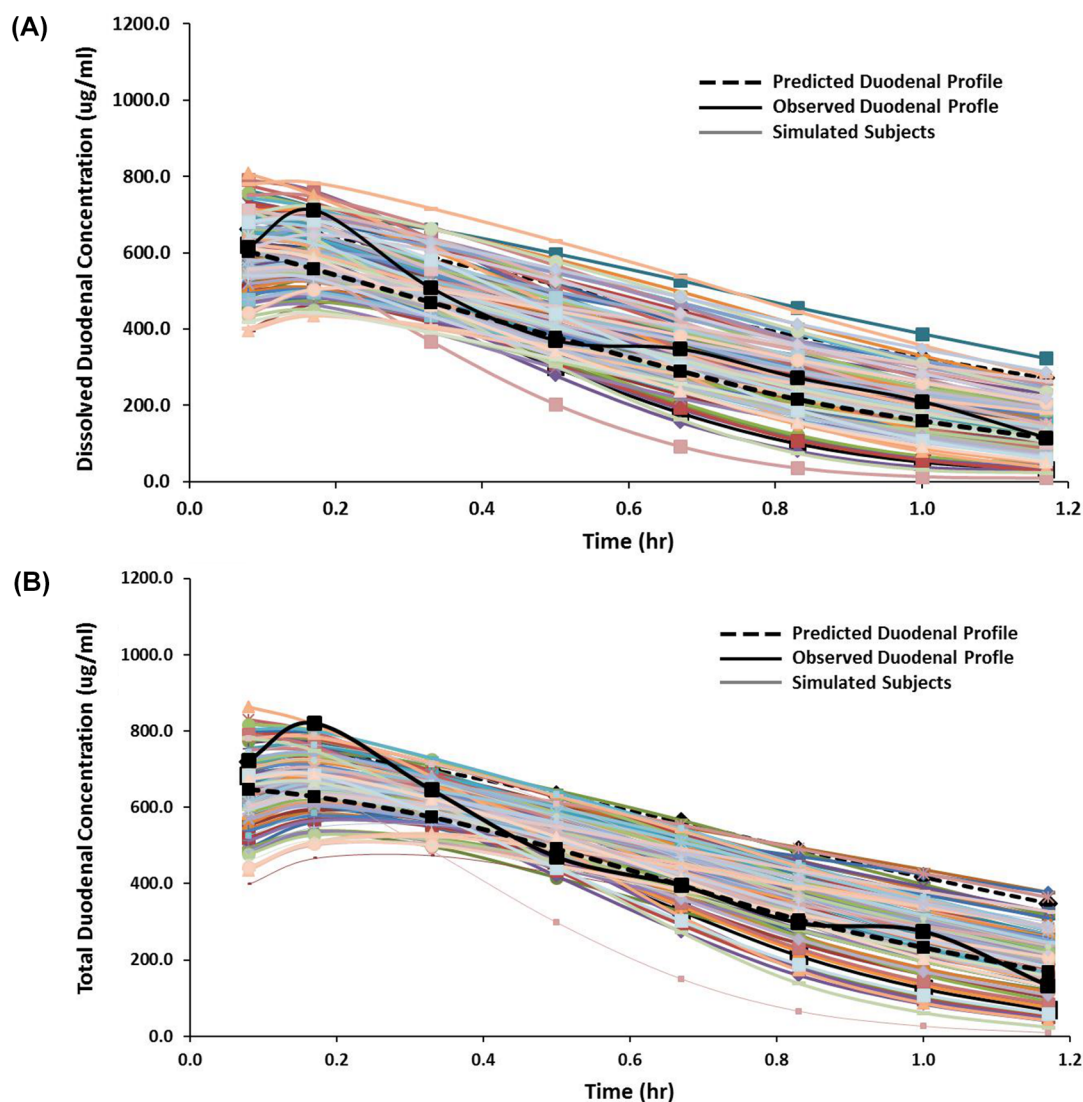


**Figure 9.** (A) Mean predicted and observed duodenal dissolved ketoconazole concentrations (data for all 120 simulated virtual subjects also plotted for the reference). (B) Mean predicted and observed duodenal total ketoconazole concentrations (data for all 120 simulated virtual subjects also plotted for the reference).

of KTZ were comparable to the corresponding observed profile values of  $520.42 \mu\text{g h mL}^{-1}$  and  $434.68 \mu\text{g h mL}^{-1}$ , respectively. The overall shapes of the duodenal profiles observed and predicted were also similar. The mean precipitated fraction ( $\pi$ ), calculated as a grand average at 30 min post administration, was found to be 0.15 compared to the *in vivo* value of 0.16 reported by Psachoulias et al.<sup>42</sup>

#### Prediction of Systemic Plasma Concentration Profiles.

Psachoulias et al. evaluated the precipitation attributes of KTZ in GI luminal fluid samples at 300 mg dose; however, their clinical study protocol did not measure the systemic exposure in parallel from same volunteers. The *in vitro* transfer experiments were conducted at 200 mg dose and compared with the luminal profile data<sup>42</sup> at 300 mg dose. Therefore, in order to further verify the suitability of the model, additional human clinical studies (oral doses ranging from 200 to 400 mg) were identified from the published literature and simulated with the appropriate trial design (Table 4).

The model reproduced the effect of supersaturation and precipitation on systemic exposure of the 200 mg IR tablet formulations very well (Table 5). The % prediction errors (%

PE) for  $C_{\text{max}}$  and  $\text{AUC}_{0-t}$  against corresponding observed clinical values were less than 25% across all tested studies. The ability of the model to predict the PK of a 400 mg IR tablet dose of KTZ (after Daneshmend et al.<sup>64</sup>) using corresponding clearance values was also studied and found comparable to the clinical profiles (Figure 10). As the simulations were able to predict the observed PK data well for multiple dosage strengths, it suggests that an increase in dose “may” not have significant effect on the precipitation kinetics, probably, due to the lower precipitation and high permeation (predicted jejunal  $P_{\text{eff}} = 3.76 \times 10^{-4} \text{ cm/s}$ ) of this API. Of course, there is an identifiability issue here which may warrant more *in vitro* and *in vivo* studies to establish the dose related changes in precipitation kinetics parameters. Additionally, it also can be noted that Psachoulias et al.<sup>42</sup> estimated the precipitated fractions at two different dose levels, 100 mg and 300 mg, which brackets the simulated dose of 200 mg in our study. The maximum precipitated fractions at 30 min were  $0.11 \pm 0.15\%$  and  $0.16 \pm 0.26\%$ , respectively, but with SD associated with the values’ small study size ( $n = 12$ ), the difference between both values is statistically insignificant.

**Table 5. Observed and Predicted Drug Exposure PK Parameters for 200 mg IR Tablet Formulations of Ketoconazole**

PK param	obsd, <sup>a</sup> mean ± SD	obsd, <sup>b</sup> mean	predicted, <sup>a</sup> mean ± SD (% PE <sup>c</sup> )	predicted, <sup>b</sup> mean (% PE <sup>c</sup> )
Mannisto et al. <sup>49</sup>				
$C_{max}$ ( $\mu\text{g}/\text{mL}$ )	4.05 ± 0.32	2.88	3.52 ± 0.96 (-13.09%)	3.41 (18.40%)
$T_{max}$ (h)	1.40 ± 0.10	1.52	0.89 ± 0.18	0.87
AUC ( $\mu\text{g h}/\text{mL}$ )	14.38 ± 2.21	13.37	11.69 ± 4.98 (23.01%)	11.69 (-12.57%)
Daneshmend et al. <sup>64</sup>				
$C_{max}$ ( $\mu\text{g}/\text{mL}$ )	4.36 ± 0.54	3.18	3.65 ± 0.92 (-16.28%)	3.56 (11.95%)
$T_{max}$ (h)	1.57 ± 0.25	1.53	0.91 ± 0.18	0.9
AUC ( $\mu\text{g h}/\text{mL}$ )	12.9 ± 1.50	12.2	12.03 ± 5.13 (-6.74%)	12.03 (-1.39%)
Huang et al. <sup>51</sup>				
$C_{max}$ ( $\mu\text{g}/\text{mL}$ )	4.22 ± 2.47	3.26	3.52 ± 0.88 (-16.59%)	3.44 (5.52%)
$T_{max}$ (h)	1.70 ± 0.90	2	0.93 ± 0.17	0.91
AUC ( $\mu\text{g h}/\text{mL}$ )	14.74 ± 8.48	14.74	11.83 ± 4.93 (-19.74%)	-19.74%

<sup>a</sup>Mean of individual volunteer PK parameters. <sup>b</sup>PK parameter values obtained from mean drug concentration vs time profile. <sup>c</sup>% PE = (predicted mean - observed mean)/(observed mean) × 100.

While there is consistent negative trend in % PE of kinetic parameters of KTZ across all the clinical studies, the error is relatively small (<25%) considering the known population variability of KTZ PK. It is important to note that the PBPK models were not optimized against the clinical studies described herein. Model predictions can of course be improved by optimizing (fitting) parameters to accurately match the *in vivo* clinical data where available. However, the main purpose of this study is to demonstrate, with examples, the use of stepwise bottom-up biopharmaceutic *IVIV\_E* modeling approach, so no further optimization of the models was undertaken.

Dose proportionality studies (Huang et al.<sup>51</sup>) suggest that CL/F decreases as dose is increased and hence the appropriate clearance values, obtained from an in-house established and validated compound database available within the Simcyp inhibitor library, were used to simulate the higher doses. Whether this nonlinearity is via a capacity-limited hepatic

uptake/metabolic mechanism or is due to a change in the tissue distribution pattern of KTZ due to changes in tissue or plasma protein binding (or both or other mechanisms) at higher doses than 400 mg remains to be fully investigated.<sup>51</sup> Hence, caution is recommended when extrapolating the developed model to simulate higher doses.

## DISCUSSION

For immediate release formulations of orally dosed drugs there are several approaches implemented within PBPK models for determining or specifying *in vivo* dissolution rate. One approach is to directly use an *in vitro* dissolution profile (or profiles) as input to the simulations. This approach is most reasonable where dissolution rate is not sensitive to variability in physiological conditions (pH, bile salt concentrations, fluid volumes, etc.) in the gastrointestinal tract, which is most likely to be the case for BCS I drugs (highly soluble, highly permeable). However, for low solubility drugs (BCS II/IV) this is much less likely to be true unless an appropriate formulation strategy is applied. It is of interest to provide tools to be able to anticipate *in vivo* dissolution rate both in an average subject and in a population of individuals where there may be significant between-subject variability in PK linked wholly or partly to interindividual variability of dissolution rate and associated factors such as solubility, buffer capacity, fluid volumes, etc. In addition to interindividual variability there are regional differences in physiological parameters to which dissolution rate may be sensitive; exposure time of the drug product to a given regional environment is linked to gastric emptying rate and (regional) intestinal residence times which themselves exhibit significant interindividual variability (and interoccasion variability). The term “variability” refers to regional differences as well as between-subject differences in each of the 9 gut regions.

Thus, for a drug (product) sensitive to such considerations, a single dissolution profile measured *in vitro* under a single set of conditions cannot be representative of the range of conditions expected *in vivo*. One could of course generate an *in vitro* dissolution profile for the stomach, one or more regions of the small intestine, and the colon (if applicable), but these will have no link to intersubject variability. One approach to this problem is to perform the *in vitro* test under mean conditions and at the extremes expected *in vivo*. However, this method does not give

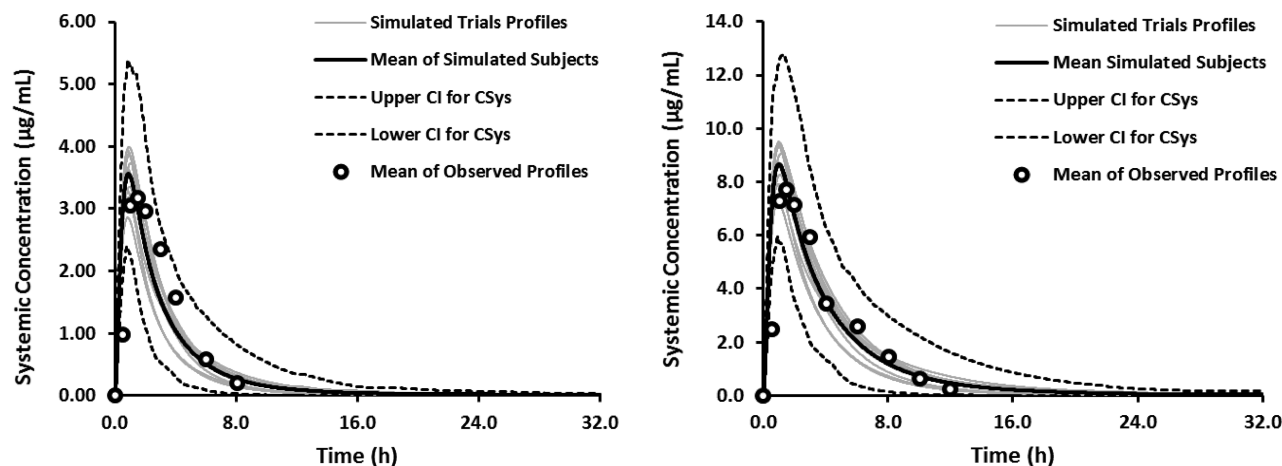


**Figure 10.** Simulated versus observed mean plasma concentration–time profiles of KTZ after single oral dose of 200 mg and 400 mg of KTZ. Ten virtual trials were simulated based on trial design and age/sex after Daneshmend et al.<sup>64</sup>



an indication of the likelihood of outcomes in a given set of individuals drawn from a population distribution.

An alternative approach is to use mechanistic models of dissolution (and solubility) which can pick up the impact of variations in physiological parameters and propagate these PK outcomes across a range of individuals. The ADAM model uses an amended Wang and Flanagan equation (eq 4) to predict particle dissolution that allows incorporation of physiological variability in luminal pH, luminal fluid volume, residence time, bile salt concentration, etc., to which the drug/dosage form is exposed during GI transit. With the particle motion model (not used in this study but now available in Simcyp)  $h_{\text{eff}}$  is linked to particle size, fluid velocity, fluid density, and  $D_{\text{eff}}$ . Alternative methods such as the Z-factor<sup>52</sup> approach lump many of the parameters of eq 4 into a single parameter ( $Z$ ) which always has to be estimated from the available dissolution data. As a result the Z-factor has no link (sensitivity) to the variability of physiological parameters, or, put another way, the model cannot extrapolate to different conditions.

It is possible with a series of *in vitro* experiments in appropriate media to estimate  $Z$  for each region, or several regions, of the GI tract and apply these values to *in vivo* simulations. However, this approach, while probably satisfactory for a representative (average individual), still does not address between-subject variability of gut physiological parameters which, particularly for BCS II and IV drugs, may result in significant variability in absorption rate and thence overall PK. In eq 4,  $S$  (the DLM scalar) is a multiplier which, if required, can be estimated through fitting, but for the reasons given we have retained the other mechanistic aspects of the diffusion model. An estimated  $S$  (or Z-factor) is of course a lumped parameter, and, while one might consider it to be a shape factor or a scalar to represent reduced surface area where particles aggregate, it may account for any mechanistic aspect not captured correctly by the model. Hence, the use of DLM scalar is not encouraged for biopharmaceutic *IVIV\_E* purposes unless its necessity can be related to a mechanism missing from the model or where there is great confidence in the required parameters (PSD,  $D_{\text{eff}}$  etc.) and therefore no obvious reason to assign lack of model predictive performance to one or several of these parameters.

The performance, assumptions, and parametrization (e.g., particle size information) of such models can be assessed through first modeling *in vitro* experiments where conditions are known (or controlled) prior to applying such models within *in vivo* simulations with PBPK models. In principle this approach may mean that *in vitro* dissolution conditions do not have to be an exact match to *in vivo* conditions since the models are able to account for pH differences or hydrodynamic differences etc. However, this remains to be demonstrated and probably requires improved characterization of *in vivo* conditions particularly in relation to hydrodynamics, for example.

*In vitro–in vivo* extrapolation approaches, although relatively new to the biopharmaceutics field, have been successfully combined with PBPK modeling to predict drug metabolism and to a lesser extent transport kinetics.<sup>53–55</sup> Overall, the stepwise approach presented herein provides a mechanistic framework for handling *in vitro* solubility, disintegration, dissolution, and precipitation experiments, permitting the confirmation and/or estimation of drug-specific parameters (viz., salt limited solubility factors, bile micelle partition coefficients, supersaturation, and precipitation related values)

required to simulate the *in vivo* behavior of the API. Performance assessment of these models directly within PBPK frameworks and their ability to accurately simulate intestinal drug dissolution/precipitation can be confounded by a multitude of factors affecting the drug absorption process. Consequently, assessment of mechanistic absorption models, and herein the accompanying *IVIV\_E* strategy, using plasma concentration profiles and derived PK parameters as the comparators is challenging.<sup>30</sup> The proposed approach can be used to assess the model performance for various *in vitro* experiments including the USP 2 and USP IV dissolution and transfer experiments and if required improve its prediction performance by measuring or estimating unknown or uncertain parameters. Although this process may be hindered by issues of parameter identifiability, this can in some instances be ameliorated through simultaneous fit across multiple different experiments.

In terms of the handling of supersaturation and precipitation, the described approach is semimechanistic, essentially mapping the characteristics of a concentration–time profile measured in the receiver (duodenal) compartment of an *in vitro* system to *in vivo*. Nonetheless, the use of a critical supersaturation concentration below which precipitation does not occur (unless precipitation has already begun) means that the variability in dissolved API concentration between individuals and in different regions of the GIT is considered. The variability built into the models in terms of gastric emptying times, duodenal (or other segment) transit time, fluid volumes, gut wall permeation rate, and other factors is accounted for when simulating the time-dependent concentration of API in the luminal fluids. The use of first-order rate constants to characterize precipitation rate has the disadvantage that the mass deposition (particle growth) rate is not sensitive to particle size and other factors such as hydrodynamics. On the other hand, use of a more mechanistic model of particle growth requires knowledge, or prediction, of the numbers and sizes of particles present, which is usually not experimentally available. Classical nucleation theory (CNT) is in principle able to predict nucleation rate but has some major limitations.<sup>56,57</sup> These include the assumptions of the capillary approximation and homogeneous nucleation together with the inherent inability to deal with the LLPS phenomenon which occurs when the amorphous solubility is exceeded.<sup>58</sup> Erdemir et al.<sup>57</sup> have described in detail the limitations of CNT and have emphasized the need for further research; the nucleation of solids from solution does not proceed via the classical pathway, but instead follows more complex routes.<sup>57</sup> Overall there are few reports of successful modeling of nucleation and precipitation within a PBPK framework<sup>59–62</sup> and there is not a standardized approach available in terms of either the *in vitro* experiments required or a suitable mechanistic framework for the *in silico* modeling.

Predictive models based purely on mechanistic rationales are certainly of great interest in a “bottom-up” *IVIV\_E* approach. These advanced models, however, have an advantage over “empirical” models, provided that the required parameters are experimentally available or can be estimated using mechanistic frameworks such the SIVA toolkit. In terms of the clinical studies, against which to evaluate and potentially refine *in vitro* and *in silico* strategies, the increasing availability of drug concentrations measured in both gastrointestinal fluids and plasma is of great benefit<sup>42,43</sup> and certainly provides an opportunity to compare these empirical vs mechanistic

approaches and their probable applications in PBPK modeling studies.

To a great extent, drug product development is still an empirical process and is often based on trial and error and can be highly dependent on the experience of the formulation scientist, with little input from predictive *in vitro* and *in silico* modeling tools.<sup>63</sup> The proposed approach can help formulation scientists to simulate and better understand the effect of critical parameters on drug behavior. A systematic modeling approach may enable selection of the most informative *in vitro* experiments and help identify the optimum biorelevant conditions for the drug product, ultimately accelerating product development in a systematic way. Such an approach can also help formulation scientists to assess the impact of drug product characteristics such as particle size, drug precipitation parameters, etc. on pharmacokinetic properties, generally unavailable in the early product development stages. Moreover, this approach streamlines the designing of informative *in vitro* experiments while omitting redundant methods, potentially reducing the cost and time of product development. At the same time it is acknowledged that further developments are required in terms of mechanistic understanding and modeling of the impact of excipient effects upon solubility, dissolution, and supersaturation and precipitation properties. The tools described form the basis for such developments.

The approach described herein has performed reasonably well at simulating the *in vivo* concentrations in luminal fluids and for a separate set of studies the clinical plasma profiles with a range of different doses. The results of this study demonstrate that the proposed stepwise *IVIV\_E* approach can help build confidence in the quality of the input parameters and assumptions of the mechanistic models used for *in vivo* simulations, with the ultimate aim to improve prediction performance of PBPK modeling tools. However, this integrated *IVIV\_E*, a “bottom-up” approach within PBPK framework, is still in its infancy, and further studies are needed to improve the confidence in the methodology.

## AUTHOR INFORMATION

### Corresponding Author

\*Tel: +44 (0) 114 292 2323. Fax: +44 (0) 114 292 2333. E-mail: [shriram.pathak@certara.com](mailto:shriram.pathak@certara.com).

### ORCID

Shriram M. Pathak: 0000-0002-3398-8890

### Notes

The authors declare the following competing financial interest(s): Shriram Pathak, Nikunj Kumar Patel, David B. Turner, and Masoud Jamei are all employees of Simcyp Limited (A Certara Company).

## ACKNOWLEDGMENTS

This work was partly supported by funding from European IMI OrBiTO Grant No. 115369 (<http://www.imi.europa.eu>). The Simcyp Simulator is freely available, following completion of the training workshop, to approved members of academic institutions and other not-for-profit organizations for research and teaching purposes. The help of Eleanor Savill and Rosalie Bower (Simcyp Limited, U.K.) in preparing the manuscript is highly appreciated.

## REFERENCES

- (1) Wagner, C.; Zhao, P.; Pan, Y.; Hsu, V.; Grillo, J.; Huang, S. M.; Sinha, V. Application of Physiologically Based Pharmacokinetic (PBPK) Modeling to Support Dose Selection: Report of an FDA Public Workshop on PBPK. *CPT: Pharmacometrics Syst. Pharmacol.* **2015**, *4*, 226–230.
- (2) Kostewicz, E. S.; Aarons, L.; Bergstrand, M.; Bolger, M. B.; Galetin, A.; Hatley, O.; Jamei, M.; Lloyd, R.; Pepin, X.; Rostami-Hodjegan, A.; Sjogren, E.; Tannergren, C.; Turner, D. B.; Wagner, C.; Weitschies, W.; Dressman, J. PBPK models for the prediction of *in vivo* performance of oral dosage forms. *Eur. J. Pharm. Sci.* **2014**, *57*, 300–321.
- (3) Margolskee, A.; Darwich, A. S.; Pepin, X.; Pathak, S. M.; Bolger, M. B.; Aarons, L.; Rostami-Hodjegan, A.; Angstenberger, J.; Graf, F.; Laplanche, L.; Muller, T.; Carlert, S.; Daga, P.; Murphy, D.; Tannergren, C.; Yasin, M.; Greschat-Schade, S.; Muck, W.; Muenster, U.; van der Mey, D.; Frank, K. J.; Lloyd, R.; Adriaenssen, L.; Bevernage, J.; De Zwart, L.; Swerts, D.; Tistaert, C.; Van Den Bergh, A.; Van Peer, A.; Beato, S.; Nguyen-Trung, A. T.; Bennett, J.; McAllister, M.; Wong, M.; Zane, P.; Ollier, C.; Vicat, P.; Kollmann, M.; Marker, A.; Brun, P.; Mazuir, F.; Beilles, S.; Venczel, M.; Boulenc, X.; Loos, P.; Lennernas, H.; Abrahamsson, B. IMI - oral biopharmaceutics tools project - evaluation of bottom-up PBPK prediction success part 1: Characterisation of the OrBiTo database of compounds. *Eur. J. Pharm. Sci.* **2017**, *96*, 598–609.
- (4) Sager, J. E.; Yu, J.; Ragueneau-Majlessi, I.; Isoherranen, N. Physiologically Based Pharmacokinetic (PBPK) Modeling and Simulation Approaches: A Systematic Review of Published Models, Applications, and Model Verification. *Drug Metab. Dispos.* **2015**, *43*, 1823–1837.
- (5) Poggesi, I.; Snoeys, J.; Van Peer, A. The successes and failures of physiologically based pharmacokinetic modeling: there is room for improvement. *Expert Opin. Drug Metab. Toxicol.* **2014**, *10*, 631–635.
- (6) Jamei, M. Recent Advances in Development and Application of Physiologically-Based Pharmacokinetic (PBPK) Models: a Transition from Academic Curiosity to Regulatory Acceptance. *Curr. Pharmacol. Rep.* **2016**, *2*, 161–169.
- (7) European Medical Agency (2016). *Guideline on the qualification and reporting of physiologically based pharmacokinetic (PBPK) modelling and simulation* (Available at [http://www.ema.europa.eu/docs/en\\_GB/document\\_library/Scientific\\_guideline/2016/07/WC500211315.pdf](http://www.ema.europa.eu/docs/en_GB/document_library/Scientific_guideline/2016/07/WC500211315.pdf)).
- (8) U.S. Department of Health and Human Services; Food and Drug Administration (FDA); Center for Drug Evaluation and Research (CDER) (2016). *Physiologically Based Pharmacokinetic Analyses-Format and Content: Guidance for Industry* (Available at <http://www.fda.gov/downloads/Drugs/GuidanceComplianceRegulatoryInformation/Guidances/UCMS531207.pdf>).
- (9) European Medical Agency (2014). *Concept paper on qualification and reporting of physiologically-based pharmacokinetic (PBPK) modelling and analyses* (Available at [http://www.ema.europa.eu/docs/en\\_GB/document\\_library/Scientific\\_guideline/2014/06/WC500169452.pdf](http://www.ema.europa.eu/docs/en_GB/document_library/Scientific_guideline/2014/06/WC500169452.pdf)).
- (10) Zhang, X.; Lionberger, R. A.; Davit, B. M.; Yu, L. X. Utility of physiologically based absorption modeling in implementing Quality by Design in drug development. *AAPS J.* **2011**, *13*, 59–71.
- (11) Kambayashi, A.; Blume, H.; Dressman, J. Understanding the *in vivo* performance of enteric coated tablets using an *in vitro-in silico-in vivo* approach: case example diclofenac. *Eur. J. Pharm. Biopharm.* **2013**, *85*, 1337–1347.
- (12) Kesisoglou, F.; Mitra, A. Application of Absorption Modeling in Rational Design of Drug Product Under Quality-by-Design Paradigm. *AAPS J.* **2015**, *17*, 1224–1236.
- (13) Jiang, W.; Kim, S.; Zhang, X.; Lionberger, R. A.; Davit, B. M.; Conner, D. P.; Yu, L. X. The role of predictive biopharmaceutical modeling and simulation in drug development and regulatory evaluation. *Int. J. Pharm.* **2011**, *418*, 151–160.
- (14) Mistry, B.; Patel, N.; Jamei, M.; Rostami-Hodjegan, A.; Martinez, M. N. Examining the Use of a Mechanistic Model to

Generate an In Vivo/In Vitro Correlation: Journey Through a Thought Process. *AAPS J.* **2016**, *18*, 1144–1158.

(15) Kesisoglou, F.; Xia, B.; Agrawal, N. G. Comparison of Deconvolution-Based and Absorption Modeling IVIVC for Extended Release Formulations of a BCS III Drug Development Candidate. *AAPS J.* **2015**, *17*, 1492–1500.

(16) Patel, N.; Polak, S.; Jamei, M.; Rostami-Hodjegan, A.; Turner, D. B. Quantitative prediction of formulation-specific food effects and their population variability from in vitro data with the physiologically-based ADAM model: a case study using the BCS/BDDCS Class II drug nifedipine. *Eur. J. Pharm. Sci.* **2014**, *57*, 240–249.

(17) Heimbach, T.; Xia, B.; Lin, T. H.; He, H. Case studies for practical food effect assessments across BCS/BDDCS class compounds using in silico, in vitro, and preclinical in vivo data. *AAPS J.* **2013**, *15*, 143–158.

(18) Parrott, N.; Lukacova, V.; Fraczkiwicz, G.; Bolger, M. B. Predicting pharmacokinetics of drugs using physiologically based modeling—application to food effects. *AAPS J.* **2009**, *11*, 45–53.

(19) Cristofolletti, R.; Dressman, J. B. Use of physiologically based pharmacokinetic models coupled with pharmacodynamic models to assess the clinical relevance of current bioequivalence criteria for generic drug products containing Ibuprofen. *J. Pharm. Sci.* **2014**, *103*, 3263–3275.

(20) Mitra, A.; Kesisoglou, F.; Dogterom, P. Application of absorption modeling to predict bioequivalence outcome of two batches of etoricoxib tablets. *AAPS PharmSciTech* **2015**, *16*, 76–84.

(21) Kortejarvi, H.; Urtti, A.; Yliperttula, M. Pharmacokinetic simulation of biowaiver criteria: the effects of gastric emptying, dissolution, absorption and elimination rates. *Eur. J. Pharm. Sci.* **2007**, *30*, 155–166.

(22) Jamei, M.; Marciniak, S.; Feng, K.; Barnett, A.; Tucker, G.; Rostami-Hodjegan, A. The Simcyp population-based ADME simulator. *Expert Opin. Drug Metab. Toxicol.* **2009**, *5*, 211–223.

(23) Rostami-Hodjegan, A.; Tucker, G. T. Simulation and prediction of in vivo drug metabolism in human populations from in vitro data. *Nat. Rev. Drug Discovery* **2007**, *6*, 140–148.

(24) Proctor, N. J.; Tucker, G. T.; Rostami-Hodjegan, A. Predicting drug clearance from recombinantly expressed CYPs: intersystem extrapolation factors. *Xenobiotica* **2004**, *34*, 151–178.

(25) Howgate, E. M.; Rowland Yeo, K.; Proctor, N. J.; Tucker, G. T.; Rostami-Hodjegan, A. Prediction of in vivo drug clearance from in vitro data. I: impact of inter-individual variability. *Xenobiotica* **2006**, *36*, 473–497.

(26) Rostami-Hodjegan, A. Physiologically based pharmacokinetics joined with in vitro-in vivo extrapolation of ADME: a marriage under the arch of systems pharmacology. *Clin. Pharmacol. Ther.* **2012**, *92*, 50–61.

(27) Jamei, M.; Turner, D.; Yang, J.; Neuhoff, S.; Polak, S.; Rostami-Hodjegan, A.; Tucker, G. Population-based mechanistic prediction of oral drug absorption. *AAPS J.* **2009**, *11*, 225–237.

(28) Margolskee, A.; Darwich, A. S.; Pepin, X.; Aarons, L.; Galetin, A.; Rostami-Hodjegan, A.; Carlert, S.; Hammarberg, M.; Hilgendorf, C.; Johansson, P.; Karlsson, E.; Murphy, D.; Tannergren, C.; Thorn, H.; Yasin, M.; Mazuir, F.; Nicolas, O.; Ramusovic, S.; Xu, C.; Pathak, S. M.; Korjamo, T.; Laru, J.; Malkki, J.; Pappinen, S.; Tuunainen, J.; Dressman, J.; Hansmann, S.; Kostewicz, E.; He, H.; Heimbach, T.; Wu, F.; Hoft, C.; Laplanche, L.; Pang, Y.; Bolger, M. B.; Huehn, E.; Lukacova, V.; Mullin, J. M.; Szeto, K. X.; Costales, C.; Lin, J.; McAllister, M.; Modi, S.; Rotter, C.; Varma, M.; Wong, M.; Mitra, A.; Bevernage, J.; Biewenga, J.; Van Peer, A.; Lloyd, R.; Shardlow, C.; Langguth, P.; Mishenzon, I.; Nguyen, M. A.; Brown, J.; Lennernas, H.; Abrahamsson, B. IMI - Oral biopharmaceutics tools project - Evaluation of bottom-up PBPK prediction success part 2: An introduction to the simulation exercise and overview of results. *Eur. J. Pharm. Sci.* **2017**, *96*, 610–625.

(29) Darwich, A. S.; Margolskee, A.; Pepin, X.; Aarons, L.; Galetin, A.; Rostami-Hodjegan, A.; Carlert, S.; Hammarberg, M.; Hilgendorf, C.; Johansson, P.; Karlsson, E.; Murphy, D.; Tannergren, C.; Thorn, H.; Yasin, M.; Mazuir, F.; Nicolas, O.; Ramusovic, S.; Xu, C.; Pathak,

S. M.; Korjamo, T.; Laru, J.; Malkki, J.; Pappinen, S.; Tuunainen, J.; Dressman, J.; Hansmann, S.; Kostewicz, E.; He, H.; Heimbach, T.; Wu, F.; Hoft, C.; Pang, Y.; Bolger, M. B.; Huehn, E.; Lukacova, V.; Mullin, J. M.; Szeto, K. X.; Costales, C.; Lin, J.; McAllister, M.; Modi, S.; Rotter, C.; Varma, M.; Wong, M.; Mitra, A.; Bevernage, J.; Biewenga, J.; Van Peer, A.; Lloyd, R.; Shardlow, C.; Langguth, P.; Mishenzon, I.; Nguyen, M. A.; Brown, J.; Lennernas, H.; Abrahamsson, B. IMI - Oral biopharmaceutics tools project - Evaluation of bottom-up PBPK prediction success part 3: Identifying gaps in system parameters by analysing In Silico performance across different compound classes. *Eur. J. Pharm. Sci.* **2017**, *96*, 626–642.

(30) Turner, D. B.; Liu, B.; Patel, N.; Pathak, S. M.; Polak, S.; Jamei, M.; Dressman, J.; Rostami-Hodjegan, A. Comment on "In Silico Modeling of Gastrointestinal Drug Absorption: Predictive Performance of Three Physiologically-Based Absorption Models". *Mol. Pharmaceutics* **2017**, *14*, 336–339.

(31) Ruff, A.; Fiolka, T.; Kostewicz, E. S. Prediction of Ketoconazole absorption using an updated in vitro transfer model coupled to physiologically based pharmacokinetic modelling. *Eur. J. Pharm. Sci.* **2017**, *100*, 42–55.

(32) Edwards, F.; Tsakmaka, C.; Mohr, S.; Fielden, P. R.; Goddard, N. J.; Booth, J.; Tam, K. Y. Using droplet-based microfluidic technology to study the precipitation of a poorly water-soluble weakly basic drug upon a pH-shift. *Analyst* **2013**, *138*, 339–345.

(33) Vertzoni, M.; Diakidou, A.; Chatzilas, M.; Soderlind, E.; Abrahamsson, B.; Dressman, J. B.; Reppas, C. Biorelevant media to simulate fluids in the ascending colon of humans and their usefulness in predicting intracolonic drug solubility. *Pharm. Res.* **2010**, *27*, 2187–2196.

(34) Glomme, A.; März, J.; Dressman, J. B. Predicting the Intestinal Solubility of Poorly Soluble Drugs. In *Pharmacokinetic Profiling in Drug Research*; Testa, B., Krämer, S. D., Wunderli-Allenspach, H., Folkers, G., Eds.; Wiley-VCH Verlag GmbH & Co. KGaA: Weinheim, Germany, 2007; pp 259–280.

(35) Avdeef, A. Physicochemical profiling (solubility, permeability and charge state). *Curr. Top. Med. Chem.* **2001**, *1*, 277–351.

(36) Al-Gousous, J.; Langguth, P. Oral Solid Dosage Form Disintegration Testing - The Forgotten Test. *J. Pharm. Sci.* **2015**, *104*, 2664–2675.

(37) Kostewicz, E. S.; Abrahamsson, B.; Brewster, M.; Brouwers, J.; Butler, J.; Carlert, S.; Dickinson, P. A.; Dressman, J.; Holm, R.; Klein, S.; Mann, J.; McAllister, M.; Minekus, M.; Muenster, U.; Mullert, A.; Verwei, M.; Vertzoni, M.; Weitschies, W.; Augustijns, P. In vitro models for the prediction of in vivo performance of oral dosage forms. *Eur. J. Pharm. Sci.* **2014**, *57*, 342–366.

(38) Kostewicz, E. S.; Wunderlich, M.; Brauns, U.; Becker, R.; Bock, T.; Dressman, J. B. Predicting the precipitation of poorly soluble weak bases upon entry in the small intestine. *J. Pharm. Pharmacol.* **2004**, *56*, 43–51.

(39) Takeuchi, S.; Tsume, Y.; Amidon, G. E.; Amidon, G. L. Evaluation of a Three Compartment In Vitro Gastrointestinal Simulator Dissolution Apparatus to Predict In Vivo Dissolution. *J. Pharm. Sci.* **2014**, *103*, 3416–3422.

(40) Indulkar, A. S.; Box, K. J.; Taylor, R.; Ruiz, R.; Taylor, L. S. pH-Dependent Liquid-Liquid Phase Separation of Highly Supersaturated Solutions of Weakly Basic Drugs. *Mol. Pharmaceutics* **2015**, *12*, 2365–2377.

(41) Galia, E.; Nicolaidis, E.; Horter, D.; Lobenberg, R.; Reppas, C.; Dressman, J. B. Evaluation of various dissolution media for predicting in vivo performance of class I and II drugs. *Pharm. Res.* **1998**, *15*, 698–705.

(42) Psachoulis, D.; Vertzoni, M.; Goumas, K.; Kalioras, V.; Beato, S.; Butler, J.; Reppas, C. Precipitation in and supersaturation of contents of the upper small intestine after administration of two weak bases to fasted adults. *Pharm. Res.* **2011**, *28*, 3145–3158.

(43) Hens, B.; Brouwers, J.; Corsetti, M.; Augustijns, P. Supersaturation and Precipitation of Posaconazole Upon Entry in the Upper Small Intestine in Humans. *J. Pharm. Sci.* **2016**, *105*, 2677–2684.



- (44) Adriana, M. M.; Stefan, R. F.; Mircea, H.; Dumitru, L.; Ionbogdan, D.; Simona, M. D. The lack of biological relevance of the official in vitro dissolution methodology for the immediate release solid oral dosage forms of ketoconazole. *Farmacia* **2011**, *59*, 853–859.
- (45) Carlson, J. A.; Mann, H. J.; Canafax, D. M. Effect of pH on disintegration and dissolution of ketoconazole tablets. *Am. J. Hosp. Pharm.* **1983**, *40*, 1334–1336.
- (46) Sadeghnia, H. R.; Hassanzadeh-Khayyat, M. Bioequivalency Study of Two Formulations of Ketoconazole Tablet in Healthy Volunteers. *Iran J. Pharm. Sci.* **2005**, *1*, 209–215.
- (47) Zhou, R.; Moench, P.; Heran, C.; Lu, X.; Mathias, N.; Faria, T. N.; Wall, D. A.; Hussain, M. A.; Smith, R. L.; Sun, D. pH-dependent dissolution in vitro and absorption in vivo of weakly basic drugs: development of a canine model. *Pharm. Res.* **2005**, *22*, 188–192.
- (48) European Medical Agency (2014). *Assessment Report: Ketoconazole HRA* (Available at [http://www.ema.europa.eu/docs/en\\_GB/document\\_library/EPAR\\_-\\_Public\\_assessment\\_report/human/003906/WC500181493.pdf](http://www.ema.europa.eu/docs/en_GB/document_library/EPAR_-_Public_assessment_report/human/003906/WC500181493.pdf)).
- (49) Mannisto, P. T.; Mantyla, R.; Nykanen, S.; Lamminsivu, U.; Ottoila, P. Impairing effect of food on ketoconazole absorption. *Antimicrob. Agents Chemother.* **1982**, *21*, 730–733.
- (50) Heel, R. C.; Brogden, R. N.; Carmine, A.; Morley, P. A.; Speight, T. M.; Avery, G. S. Ketoconazole: a review of its therapeutic efficacy in superficial and systemic fungal infections. *Drugs* **1982**, *23*, 1–36.
- (51) Huang, Y. C.; Colaizzi, J. L.; Bierman, R. H.; Woestenborghs, R.; Heykants, J. Pharmacokinetics and dose proportionality of ketoconazole in normal volunteers. *Antimicrob. Agents Chemother.* **1986**, *30*, 206–210.
- (52) Takano, R.; Sugano, K.; Higashida, A.; Hayashi, Y.; Machida, M.; Aso, Y.; Yamashita, S. Oral absorption of poorly water-soluble drugs: computer simulation of fraction absorbed in humans from a miniscale dissolution test. *Pharm. Res.* **2006**, *23*, 1144–1156.
- (53) T'Jollyn, H.; Snoeys, J.; Colin, P.; Van Bocxlaer, J.; Annaert, P.; Cuyckens, F.; Vermeulen, A.; Van Peer, A.; Allegaert, K.; Mannens, G.; Bousserly, K. Physiology-based IVIVE predictions of tramadol from in vitro metabolism data. *Pharm. Res.* **2015**, *32*, 260–274.
- (54) Chen, Y.; Jin, J. Y.; Mukadam, S.; Malhi, V.; Kenny, J. R. Application of IVIVE and PBPK modeling in prospective prediction of clinical pharmacokinetics: strategy and approach during the drug discovery phase with four case studies. *Biopharm. Drug Dispos.* **2012**, *33*, 85–98.
- (55) Jamei, M.; Bajot, F.; Neuhoff, S.; Barter, Z.; Yang, J.; Rostami-Hodjegan, A.; Rowland-Yeo, K. A mechanistic framework for in vitro-in vivo extrapolation of liver membrane transporters: prediction of drug-drug interaction between rosuvastatin and cyclosporine. *Clin. Pharmacokinet.* **2014**, *53*, 73–87.
- (56) Karthika, S.; Radhakrishnan, T. K.; Kalaichelvi, P. A Review of Classical and Nonclassical Nucleation Theories. *Cryst. Growth Des.* **2016**, *16*, 6663–6681.
- (57) Erdemir, D.; Lee, A. Y.; Myerson, A. S. Nucleation of crystals from solution: classical and two-step models. *Acc. Chem. Res.* **2009**, *42*, 621–629.
- (58) Taylor, L. S.; Zhang, G. G. Physical chemistry of supersaturated solutions and implications for oral absorption. *Adv. Drug Delivery Rev.* **2016**, *101*, 122–142.
- (59) Jakubiak, P.; Wagner, B.; Grimm, H. P.; Petrig-Schaffland, J.; Schuler, F.; Alvarez-Sanchez, R. Development of a Unified Dissolution and Precipitation Model and Its Use for the Prediction of Oral Drug Absorption. *Mol. Pharmaceutics* **2016**, *13*, 586–598.
- (60) Carlert, S.; Lennernas, H.; Abrahamsson, B. Evaluation of the use of Classical Nucleation Theory for predicting intestinal crystalline precipitation of two weakly basic BSC class II drugs. *Eur. J. Pharm. Sci.* **2014**, *53*, 17–27.
- (61) Wagner, C.; Jantravid, E.; Kesisoglou, F.; Vertzoni, M.; Reppas, C.; Dressman, J. B. Predicting the oral absorption of a poorly soluble, poorly permeable weak base using biorelevant dissolution and transfer model tests coupled with a physiologically based pharmacokinetic model. *Eur. J. Pharm. Biopharm.* **2012**, *82*, 127–138.
- (62) Sugano, K. A simulation of oral absorption using classical nucleation theory. *Int. J. Pharm.* **2009**, *378*, 142–145.
- (63) Lennernas, H.; Aarons, L.; Augustijns, P.; Beato, S.; Bolger, M.; Box, K.; Brewster, M.; Butler, J.; Dressman, J.; Holm, R.; Julia Frank, K.; Kendall, R.; Langguth, P.; Sydor, J.; Lindahl, A.; McAllister, M.; Muenster, U.; Mullertz, A.; Ojala, K.; Pepin, X.; Reppas, C.; Rostami-Hodjegan, A.; Verwei, M.; Weitschies, W.; Wilson, C.; Karlsson, C.; Abrahamsson, B. Oral biopharmaceutics tools - time for a new initiative - an introduction to the IMI project OrBiTo. *Eur. J. Pharm. Sci.* **2014**, *57*, 292–299.
- (64) Daneshmend, T. K.; Warnock, D. W.; Ene, M. D.; Johnson, E. M.; Potten, M. R.; Richardson, M. D.; Williamson, P. J. Influence of food on the pharmacokinetics of ketoconazole. *Antimicrob. Agents Chemother.* **1984**, *25*, 1–3.
- (65) Dollery, C. T. *Therapeutic Drugs*, 2nd ed.; Churchill Livingstone: London, 1999; Vol. 1.
- (66) Martinez-Jorda, R.; Rodriguez-Sasiain, J. M.; Suarez, E.; Calvo, R. Serum binding of ketoconazole in health and disease. *Int. J. Clin. Pharmacol. Res.* **1990**, *10*, 271–276.
- (67) Ingels, F.; Beck, B.; Oth, M.; Augustijns, P. Effect of simulated intestinal fluid on drug permeability estimation across Caco-2 monolayers. *Int. J. Pharm.* **2004**, *274*, 221–232.
- (68) Kalantzi, L.; Persson, E.; Polentarutti, B.; Abrahamsson, B.; Goumas, K.; Dressman, J. B.; Reppas, C. Canine intestinal contents vs. simulated media for the assessment of solubility of two weak bases in the human small intestinal contents. *Pharm. Res.* **2006**, *23*, 1373–1381.
- (69) Oh, S. Y.; McDonnell, M. E.; Holzbach, R. T.; Jamieson, A. M. Diffusion coefficients of single bile salt and bile salt-mixed lipid micelles in aqueous solution measured by quasielastic laser light scattering. *Biochim. Biophys. Acta, Lipids Lipid Metab.* **1977**, *488*, 25–35.
- (70) Cristofaletti, R.; Patel, N.; Dressman, J. B. Differences in Food Effects for 2 Weak Bases With Similar BCS Drug-Related Properties: What Is Happening in the Intestinal Lumen? *J. Pharm. Sci.* **2016**, *105*, 2712–2722.
- (71) Rodgers, T.; Rowland, M. Mechanistic approaches to volume of distribution predictions: understanding the processes. *Pharm. Res.* **2007**, *24*, 918–933.